INSTRUMENTATION OF THE TRANSONIC TURBINE TEST RIG TO DETERMINE THE PERFORMANCE OF TURBINE INLET GUIDE VANES BY THE APPLICATION OF THE MOMENTUM AND MOMENT OF MOMENTUM EQUATIONS

PATRICK MICHAEL COMMONS

INSTRUMENTATION OF THE TRANSONIC TURBINE TEST RIG TO DETERMINE THE PERFORMANCE OF TURBINE INLET GUIDE VANES BY THE APPLICATION OF THE MOMENTUM AND MOMENT OF MOMENTUM EQUATIONS

by

Patrick Michael Commons
Lieutenant, United States Navy
B.S., Naval Academy, 1959

Submitted in partial fulfillment of the
requirements for the degree of

MASTER OF SCIENCE IN AERONAUTICAL ENGINEERING

from the

NAVAL POSTGRADUATE SCHOOL
September 1967

ABSTRACT

The primary purpose of the Transonic Turbine Test Rig is to study the effects of axial and radial clearances on turbine performance. Additionally, the installation was designed to permit the determination of stator discharge velocities by the application of the momentum and moment of momentum equations.

Previous attempts to obtain stator discharge velocities by these methods have been unsuccessful. However, during this series of tests, with over 150 hours of useful operating time, the instrumentation and the data acquisition procedures were improved to the extent that the difference between stator discharge velocities obtained from a momentum analysis and those obtained from continuity were reduced to less than three percent.

Thesis by: Patrick Michael Commons entitled Instrumentation of the Transonic Turbine Test Rig to Determine the Performance of Turbine Inlet Guide Vanes by the Application of the Momentum and Moment of Momentum Equations.

ERRATA

Page	Line	Change	To
35	24/25	exhaust-er	exhaus-ter
36	24/25	dynamom-eter	dynamo-meter
71	8/9	dynam-ic	dyna-mic

TABLE OF CONTENTS

LIST OF TABLES

LIST OF ILLUSTRATIONS

TABLE OF SYMBOLS

Symbols		Fortran
a	Mean stator/rotor throat dimension (in.)	ASTAT/AROTR
A_{th}	Stator throat area ($in.^2$)	ATH
A_1	Annulus area, stator discharge ($in.^2$)	AAX
A_2	Annulus area, rotor discharge ($in.^2$)	AAXR
C_n	Constant in flow nozzle equation (dimensionless)	CN
C_1	Conversion Factor, 2gJ ($ft.^2$-lbm/$sec.^2$-BTU)	CL
C_2	Conversion Factor, $2gJc_p$ ($ft.^2/sec.^2-{}^oR$)	C2
C_3	Conversion Factor (γ -1) (dimensionless)	C3
C_4	Conversion Factor $\gamma/(\gamma$ -1) (dimensionless)	C4
C_5	Conversion Factor (lbs./$in.^2$/in.-H_20)	C5
D_n	Flow nozzle diameter (in.)	DN
D_1	Pipe diameter at flow nozzle inlet (in.)	
F_{cl}	Axial force on the closure plate (lbs.)	CLAXIL
F_i	Pressure forces on the stator assembly	F1-6
F_s	Axial force on the stator assembly (lbs.)	AXIL
g	Universal gravitational constant (ft.-lbm./$sec.^2$-lb.)	G
H	Total enthalpy (BTU/lbm.)	
H_e	Equivalent total enthalpy (BTU/lbm.)	
h	Blade height (in.)	
h	Static enthalpy (BTU/lbm.)	
h_w	Differential pressure across flow nozzle (in. H_20)	DH
HP	Horsepower	

Symbols		Fortran
J	Conversion factor (778.16 ft.-lb/BTU)	CJ
k_{is}	Head coefficient (dimensionless)	XKIS
k_t	Factor to account for stator/rotor blade trailing edge thickness (dimensionless)	SKT/RKT
M_1	Mach Number at stator discharge (dimensionless)	VMI
M	Moment (ft.-lb.)	
M_{cl}	Moment on closure plate (ft.-lb.)	CLTORQ
M_D	Dynamometer moment (ft.-lb.)	DYNA
M_s	Moment on stator assembly	TORQ
m_s	Mass flow rate (slugs/sec.)	
N	Rotational speed (RPM)	RPM
n	Polytropic exponent (dimensionless)	POLY
$\bar{n}$	Outward normal vector (dimensionless)	
p_{atm}	Manometer reference pressure (in. Hg.)	PATM
p_{bar}	Barometric pressure (in. Hg.)	PBAR
p_{hood}	Hood pressure (in. Hg.)	PHD
p_{hub}	Hub static pressure at stator discharge (in. Hg.)	PHUB
p_{noz}	Total pressure at flow nozzle inlet (in. Hg.)	PNOZ
p_{ref1} p_{ref2}	Manometer reference pressures (in. Hg.)	PRF1/PRF2
p_{spl}	Total pressure in plenum (in. Hg.)	PSPL
p_{tpl}	Total pressure at stator inlet (in. Hg.)	PTPL
p_{tip}	Tip static pressure at stator discharge (in.Hg.)	PTIP
p_{14-20}	Shroud static pressures (in. Hg.)	P14-P20

Symbols		Fortran
R	Gas constant for air (53.34 ft.-lb/lbm.^{o}R)	CR
R_{hub}	Hub radius (in.)	RHUB
R_{m}	Mean radius (in.)	RM
R_{tip}	Tip radius (in.)	RTIP
r*	Theoretical degree of reaction (dimensionless)	REAC
S	Entropy (BTU/lbm-^{o}R)	
S	Blade spacing (in.)	SSTAT/SROTR
TCL	Temperature in Cascade Lab (^{o}F)	TCL
TCR	Temperature in Control Room (^{o}F)	TCR
T_{noz}	Temperature at flow nozzle inlet (mv)	TNOZ
T_{tpl}	Temperature in plenum (mv)	TTPL
t	Blade trailing edge thickness (in)	THK
U	Peripheral velocity (ft./sec.)	U
V	Absolute velocity (ft./sec.)	V
W	Relative velocity (ft./sec.)	W
$\dot{w}_{l}$	Plenum labyrinth leakage flow rate (lbm./sec.)	FLOWL
$\dot{w}_{t}$	Turbine mass flow rate (lbm./sec.)	FLOWT
Y_{l}	Expansion factor in flow equation (dimensionless)	Y
Z	Number of blades (dimensionless)	

Greek Letters

α	Absolute discharge angle (deg.)	ALPH
α_{n}	Coefficient of thermal expansion (dimensionless)	ALPHN
β	Relative discharge angle (deg.)	BETA

Greek Letters		Fortran
β	Ratio of nozzle minimum diameter to upstream pipe dimension (dimensionless)	BETA
γ	Specific heat ratio (c_p/c_v) (dimensionless)	GAM
δ	Referred pressure ($p_{t_o}/14.7$) (dimensionless)	DEL
ζ	Loss coefficient (dimensionless)	ZETA
η	Efficiency (dimensionless)	ETA
θ	Referred temperature $T_{tp1}/518.7$ (dimensionless)	THETA
ξ	Blockage factor (dimensionless)	XI
ρ	Density (slugs/ft^3)	
Φ	Non-dimensional flow function	PHI
ϕ_l	Labyrinth seal pressure ratio function (dimensionless)	FLOWL
ω	Angular velocity (radians/sec.)	

Subscripts		
a	Axial direction	Suffix A
is	Isentropic from inlet conditions	
r	Rotor	Prefix or Suffix R
s	Stator	Prefix or Suffix S
u	Peripheral direction	Suffix U
o	Inlet to stator	
1	Stator discharge	Suffix 1
2	Rotor discharge	Suffix 2

1. Introduction.

The Ares Mod II turbine is a single stage axial flow power unit designed by Dr. M. H. Vavra of the Department of Aeronautics, U. S. Naval Postgraduate School, Monterey, California, for use as a power generating device in a liquid rocket propulsion plant requiring a small high speed unit.

Tests were conducted on a scale model of this turbine to determine the effects of axial and radial clearances on the overall turbine performance. The Transonic Turbine Test Rig, hereafter referred to as TTR, was modified to accommodate this model.

The TTR was originally designed to provide a means of determining stator performance by the application of the momentum and moment of momentum equations, as well as obtaining the effects of axial and radial clearances on turbine performance without the need for probe installations between the stator and the rotor.

The tests were performed jointly with Lt. J. A. Messegee, U.S.N. The effects of axial and radial clearances on turbine performance are described by Messegee.[1]

This thesis is concerned with the feasibility of determining stator performance by the methods mentioned above. Additionally, it describes the test installation, the test procedures and the data reduction methods for all tests performed.

---

[1]Messegee, J. A., Influence of Axial and Radial Clearances on the Performance of a Turbine Stage with Blunt Edge Non-Twisted Blades (Naval Postgraduate School, 1967), Sec. 6.

The author is most appreciative for the time spent by Dr. M. H. Vavra in providing encouragement and counsel. In addition a special expression of appreciation is due to Mr. J. Hammer who willingly spent long hours helping to acquire the vast amount of data necessary to complete the tests.

2. Test Installation.

The test installation is composed of three sections: the Allis Chalmers 12 stage axial compressor with its associated piping, the exhauster assembly (hood, nozzle, turbine hood, flow inlet section) described by Monroe,[2] and the TTR, which will be described in detail.

The Allis Chalmers compressor is the source of drive air for both the exhauster assembly and the TTR. When operated independently, the compressor discharges to the atmosphere through a discharge valve. When run in conjunction with the TTR, compressor air is discharged into a settling tank located in the test cell. The supply of compressor air to the settling tank is controlled by an electrically operated butterfly valve.

Fig. 1 depicts the piping installation for the TTR. Turbine air passes from the first settling tank into an eight in. pipe, thence through a flow nozzle into a six

---

[2]Monroe, P. A., An Investigation of the Performance and Mixing Phenomena Associated with a Supersonic Exhauster Interacting with Subsonic Secondary Flow (Naval Postgraduate School, 1967), Sec. 2.

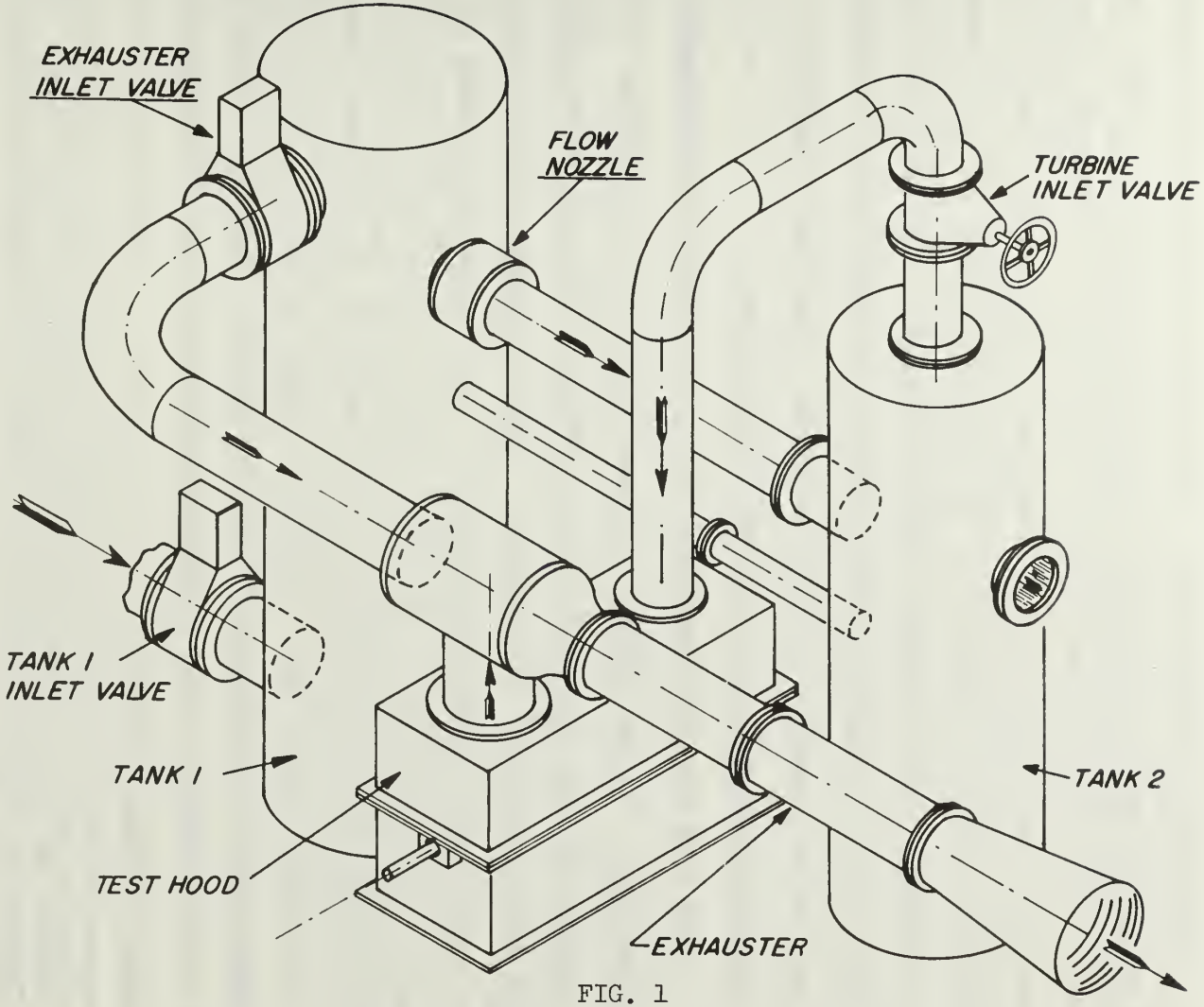

FIG. 1

PIPING INSTALLATION, TRANSONIC TURBINE TEST RIG

in. pipe discharging into a second settling tank. The flow nozzle is a non-standard flow measuring device. Therefore, nozzle calibration was necessary. This was first done by Eckert[3] and then by Naviaux.[4]

Turbine air passes from the second settling tank through a manually operated control valve into a six in. pipe leading to the TTR plenum chamber. Exhauster air passes from the first settling tank through an electrically controlled butterfly valve into a six in. pipe leading to the exhauster nozzle. The exhauster nozzle converts the airflow into a high velocity low pressure stream whose momentum is sufficient to discharge the turbine flow rate from a partial vacuum inside the hood to the atmosphere.

The TTR may be operated with or without the exhauster assembly. In the latter configuration the butterfly valve leading to the exhauster is closed and the exhauster with the hood assembly is removed. The discharge side of the TTR is then open to the atmosphere. Tests were performed in both configurations. However, at pressure ratios above 1.5 operation with the exhauster is required to maintain turbine speed within an acceptable range, primarily because of dynamometer limitations. At the higher pressure ratios the turbine inlet pressure can be reduced so that the turbine power becomes smaller.

---

[3]Eckert, R. H., Performance Analysis and Initial Tests of a Transonic Turbine Test Rig (Naval Postgraduate School, 1966), Sec. 5.

[4]Naviaux, J. C., Transonic Turbine Test Rig Exhauster System Tests and Tests of a Reaction Turbine (Naval Postgraduate School, 1966), pp. 34 and 35.

The TTR is unique inasmuch as it permits the evaluation of stator performance by the application of the momentum and moment of momentum equations. This may be done by measuring the flow conditions existing ahead of, and the forces and moments acting on, the stator. The stator assembly is free floating to permit measurement of these forces and moments.

Fig. 2 depicts the support structure for the floating stator assembly. The cradle and stator assembly are supported on the test bed by two cradle supports. The cradle is attached to these supports by four 2.5 in. aluminum thrust flexures which enable the cradle with the stator assembly to move in the axial direction without changing the radial tip clearance of the turbine rotor. The stator assembly is hanging from an aluminum cross member welded to the cradle, as shown in Fig. 2. A 0.75 in. pin, extending from the center of the cross member, fits through a bracket designed to accommodate a Fafnir Self-Aligning Rod End. To its lower end is attached a specially designed bracket with two Fafnir Track Roller type bearings. These bearings ride on the inner periphery of a circular arc fitting attached to the upper portion of the stator housing. This design permits rotation of the stator assembly about its centerline and supports its weight. Two torque flexures, extending from either side of the stator housing, transmit the thrust acting on the stator assembly to the cradle while offering little resistance to torque and

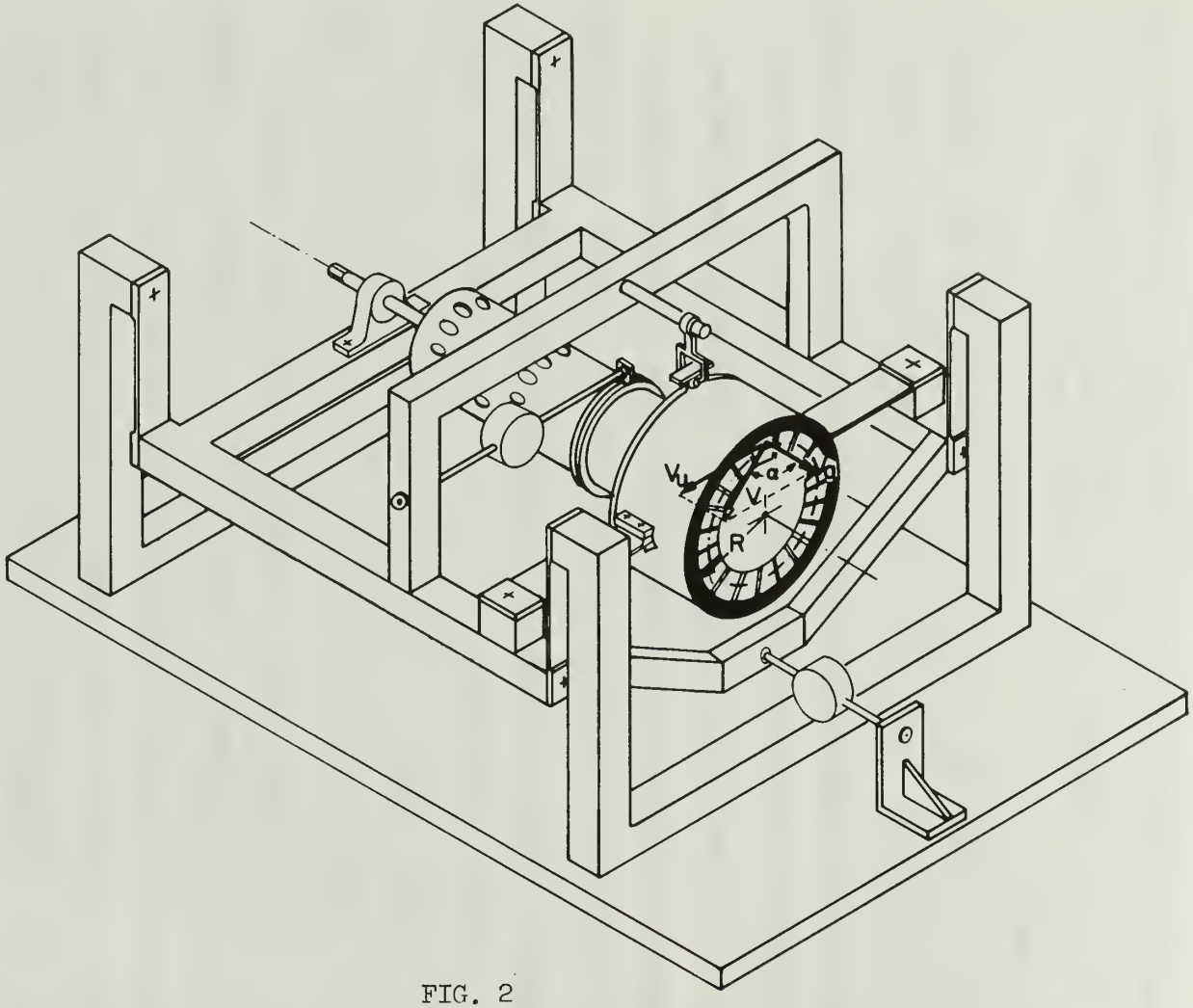

FIG. 2

FLOATING STATOR ASSEMBLY

maintain the proper alignment of the front part of the assembly. A 0.75 in. steel shaft extends from the plenum chamber. This shaft is supported by a pillow block attached to the cradle to guarantee the central alignment of the stator assembly. With the calibration stand the shaft is used also to apply known forces and moments to calibrate the force pickups used to measure the thrust and torque exerted on the stator during operation of the TTR. The force pickups used are reluctance type force capsules built by the Wiancko Engineering Company. Thrust is measured by a Model F1021 pickup with a range of 0-300 lbs. and torque by a Model F1009 pickup with a range of 0-100 lbs. The thrust pickup is mounted between the forward cross member of the cradle and a bracket affixed to the test bed. The torque pickup is attached to the weight support cross member and the plenum chamber. Fig. 3 is a scale drawing of the TTR illustrating the installation of the floating stator assembly.

The turbine rotor is attached to an overhung shaft which is supported by a separate bearing housing that is fixed to the test bed. The shaft runs in two matched sets of high-precision ball bearings that are lubricated by oil-mist. A steel quill shaft is used to connect the rotor shaft to a Vortec Air Dynamometer located outside the hood. The bearing housing may be moved axially to change the axial clearances between rotor and stator bladings from about zero to 1.5 in.

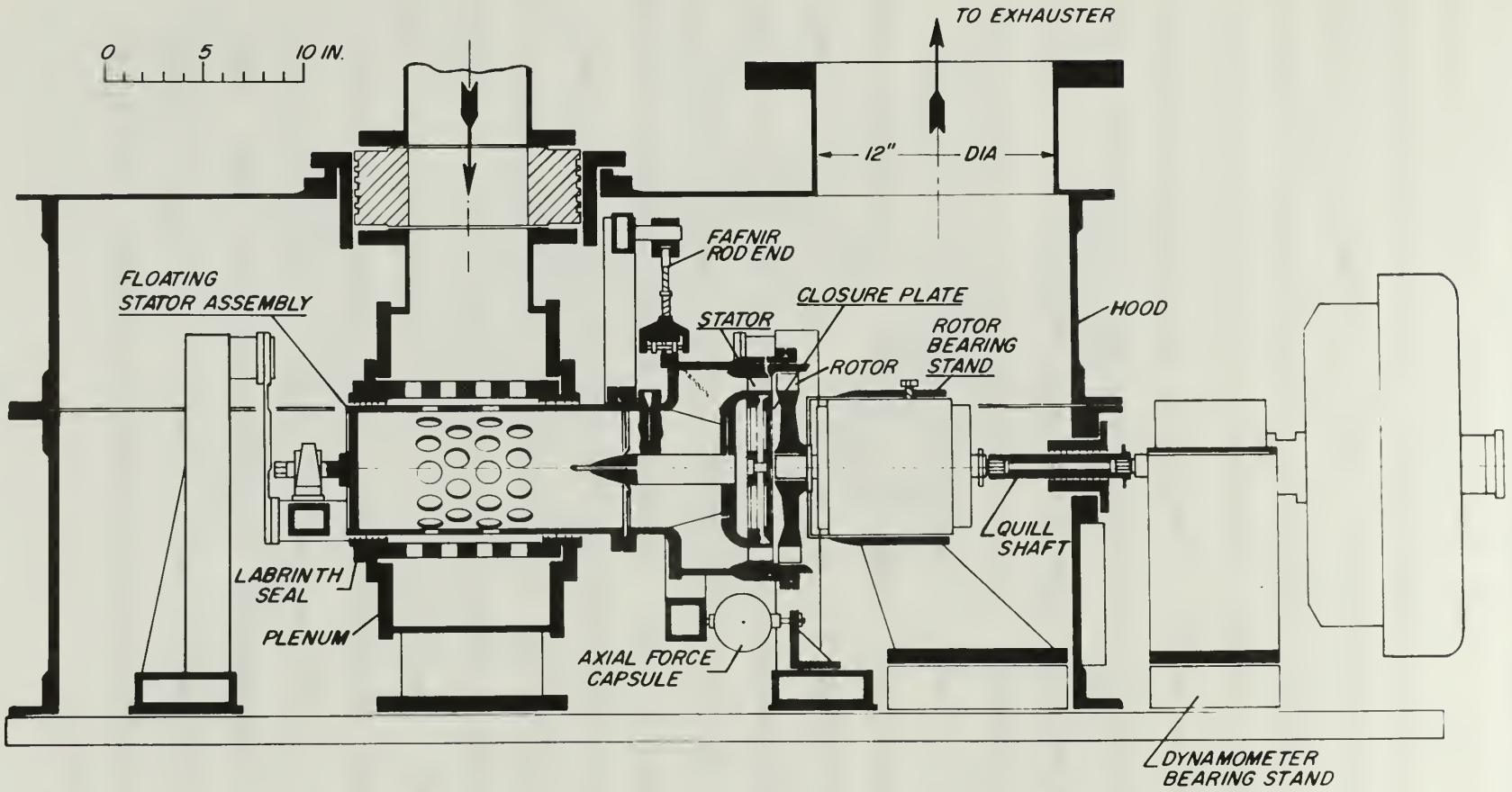

FIG. 3

TRANSONIC TURBINE TEST RIG

A six-lobe flux cutter is fitted to the end of the quill shaft outside of the hood. These lobes, in conjunction with a magnetic pickup provide a means for determining turbine speed. Turbine speed is read on a Hewlett-Packard electronic counter actuated by the pickup.

Turbine speed is controlled by varying the flow area of the dynamometer, thereby varying the load on the turbine. The dynamometer is designed so that its output torque may be measured in one of two ways, either by strain gage equipped electronic capsules or by a direct reading spring capsule. Neither of these methods proved entirely satisfactory. The electronic capsules were difficult to calibrate and repeatable results could not be obtained. This situation could be attributed to the wide temperature variations in the test cell during the tests. These temperature variations are due to high temperature air exhausting from the dynamometer. The spring capsule could only be read in the test cell. For these reasons a more reliable and temperature insensitive electronic torque measuring system was developed that could be calibrated with ease. Fig. 4 shows the installation of the measuring device that proved most satisfactory. The installation consists of a twenty in. long arm attached to the dynamometer housing which is used in conjunction with a Wiancko Model F1009 force capsule with a range of 0-50 lbs. The support structure for the force pickup consists of two aluminum extrusions attached to the test bed, with a bracket mounted between

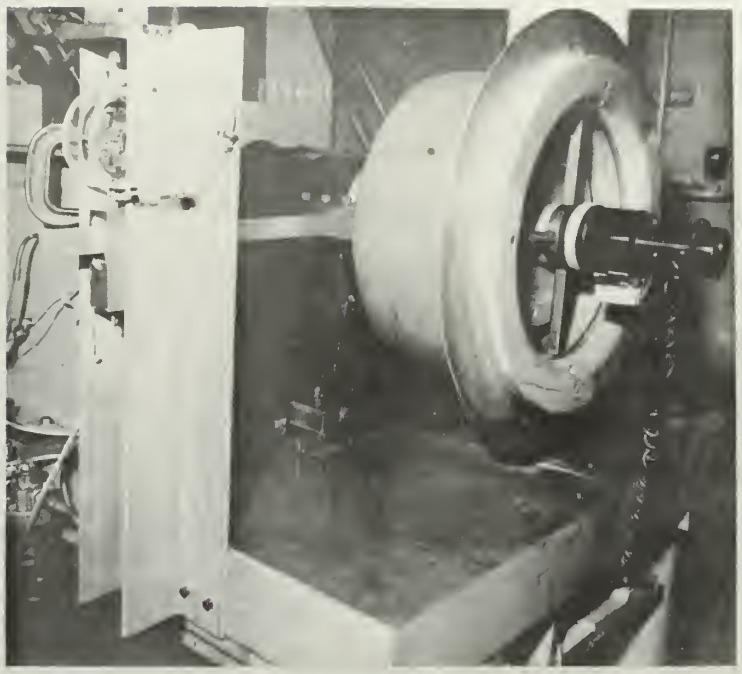

(a)

(b)

FIG. 4

TORQUE MEASURING ASSEMBLY

(a) Dynamometer, Dynamometer Arm, Force Capsule Support Structure, Force Capsule. (b) Force Capsule with Dynamometer Arm in position.

them. The force pickup is attached to a Fafnir Self-Aligning Rod End mounted in the support bracket. To the lower end of the force pickup is fitted an aluminum block, milled out to allow the free end of the dynamometer arm to pass through it. The dynamometer arm has a ball fitting attached to the free end which rests in a hemispherical groove cut in the aluminum block. The hemispherical groove has a larger radius than the ball fitting to insure proper alignment between the dynamometer arm and the force capsule. Additionally, a fitting is attached to the bottom of the aluminum block for the calibrating of the force pickup with known weights. This assembly was successful for the measuring of the dynamometer torque independent of the ambient temperature in the test cell. The torque exerted on the dynamometer housing is transmitted to the arm and produces a tension load that is taken up by the force capsule. Only tensile loading will be indicated since the dynamometer arm is not rigidly attached to the force capsule, which in turn is not rigidly attached to the support structure.

The following paragraphs describe the flow of the air through the TTR and discuss the instrumentation necessary to measure the flow properties at different locations. Air enters the plenum chamber and passes through a large number of holes into the floating stator assembly. In the fixed plenum chamber the air temperature is measured by two thermocouples that extend into the airflow from opposite sides of the plenum chamber.

The mass flow of air entering the plenum is that measured by the flow nozzle. However, the airflow through the turbine is reduced by the leakage through the plenum labyrinth seals. Methods to determine the reduction in turbine mass flow due to this leakage are given by Eckert.[5]

A special probe housing extends from the central body of the floating stator assembly. This housing, referred to as the bullet probe, contains a total and static pressure probe and a thermocouple to measure total temperature. The total pressure measured by this probe was not used in these tests due to the losses incurred between this point and the stator.

Fig. 5 is an enlarged view of the stator section shown in Fig. 3. It illustrates the installation of the Ares Mod II Turbine in the test rig. Three conical screens are arranged ahead of the stator. They were installed to insure uniform flow distribution ahead of the stator. The total pressure at the stator inlet is therefore measured by six fixed Kiel probes, equally spaced around the periphery of the stator housing. Additionally, there are arranged two radially adjustable total pressure and total temperature Kiel probes just aft of the screens, as shown in Fig. 6.

A closure plate is attached to, and concentric with, the stator. The closure plate is installed to provide a means

---

[5] Eckert, R. H., Performance Analysis and Initial Tests of a Transonic Turbine Test Rig (Naval Postgraduate School, 1966), Sec. 5.

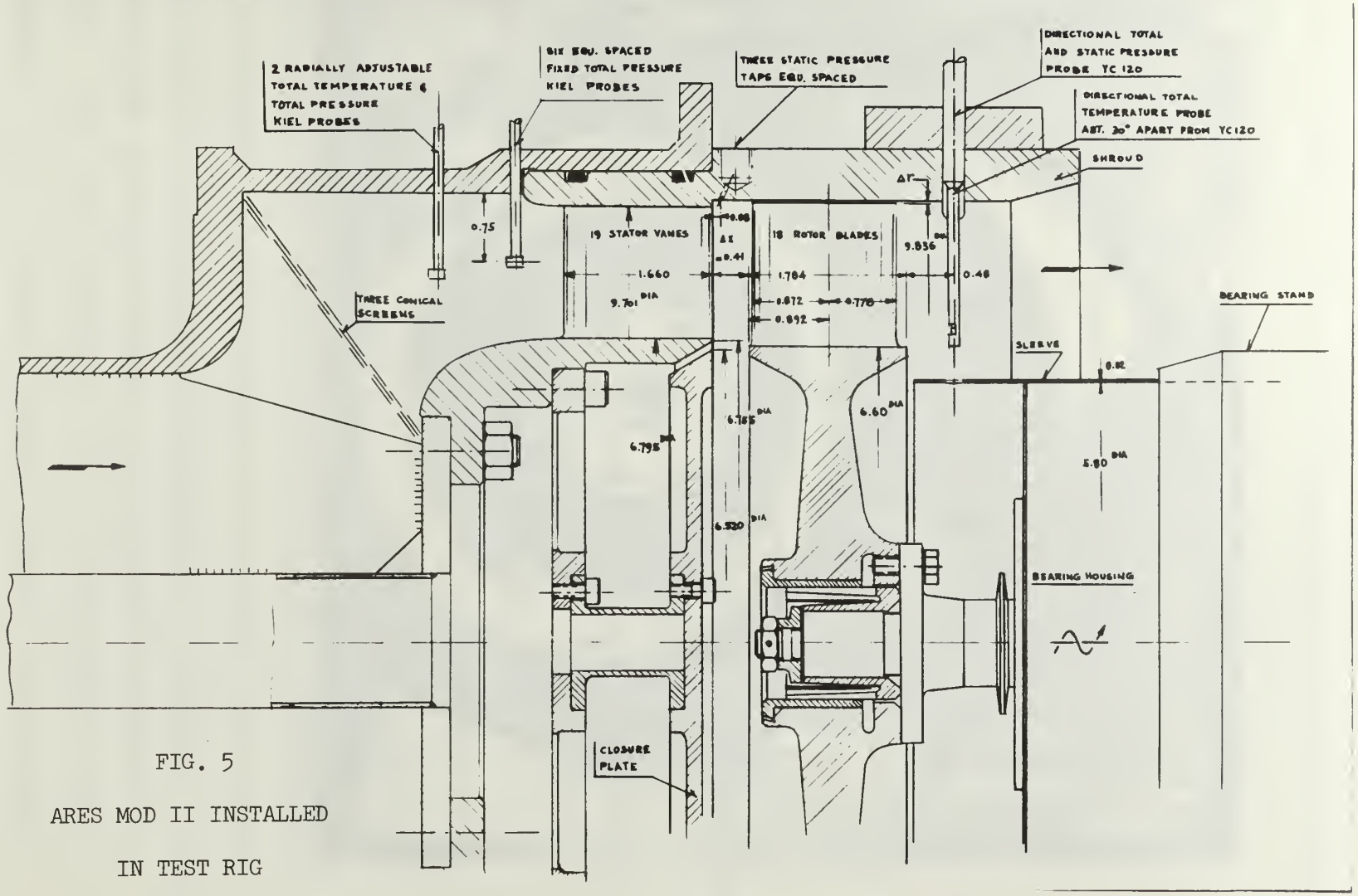

FIG. 5

ARES MOD II INSTALLED

IN TEST RIG

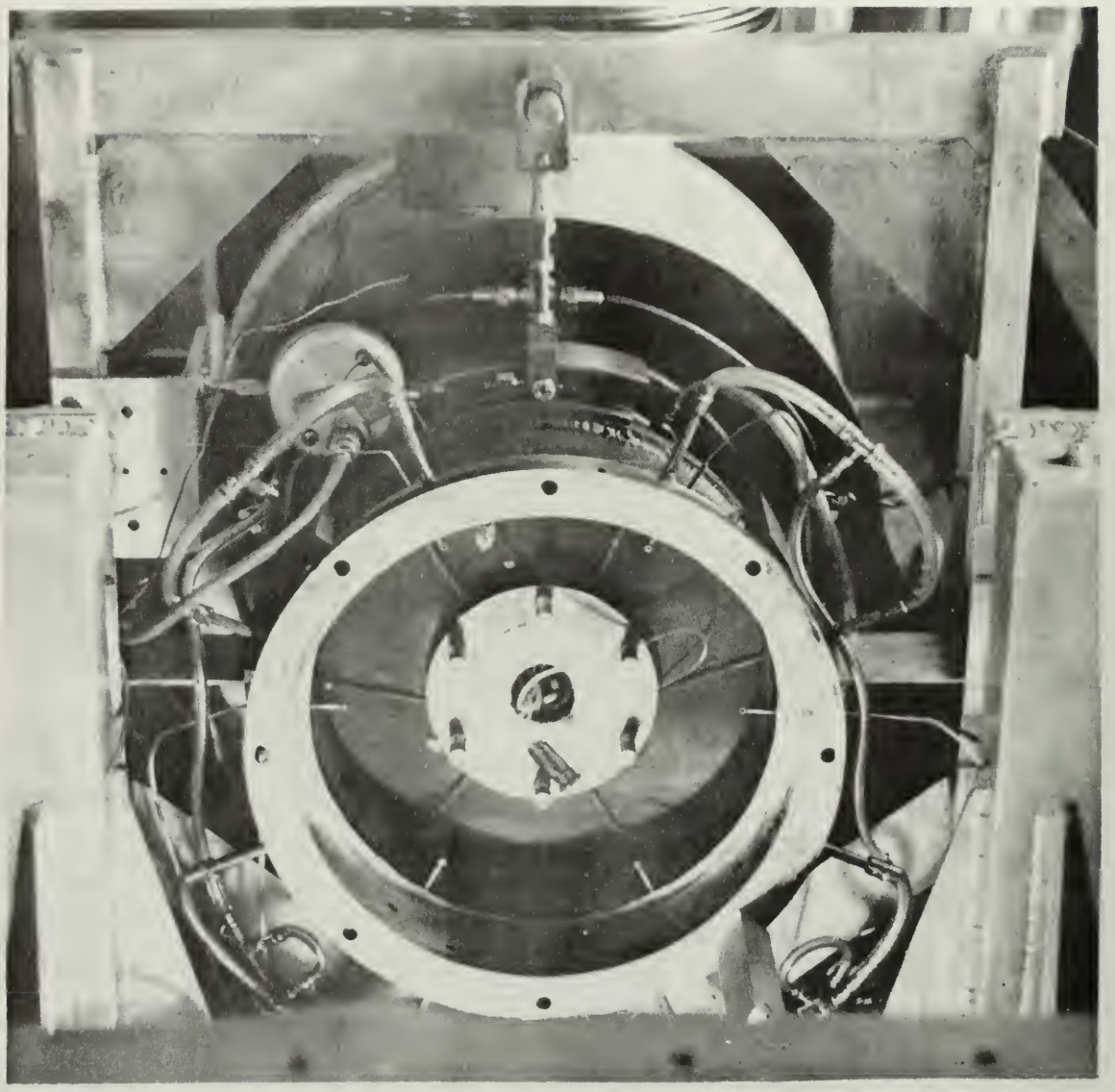

FIG. 6

STATOR INLET FLOW PASSAGE

of determining the static pressure force and moment on the stator assembly in the region between the stator hub and the turbine centerline.

Torque is exerted on the closure plate by the shear forces in the peripheral direction. These forces are the result of the rotational motion imparted to the fluid by the rotor.

The static pressure existing on the downstream side of the closure plate is different from that in the chamber behind the closure plate. Due to the rotational velocity imparted to the fluid by the rotor, the pressure on the downstream side of the closure plate varies with radius. Therefore, an accurate measurement of this pressure may not be readily obtained. However, by obtaining the force exerted on the closure plate, due to the pressure differential across it, an accurate measurement of the pressure force exerted on this area is obtained.

The closure plate is attached to a spool which in turn is attached to a spoked wheel type flexure. The spool and flexure are instrumented with strain gages to obtain the axial force and torque on the closure plate. The pressure in the chamber formed by the bullet probe support, stator and closure plate, p_{hub}, is measured on a manometer board with tubes that pass through the supports of the bullet probe. Then the net force on the closure plate is that caused by p_{hub}, less the measured force on the closure plate.

Initial tests were run with a three-spoke flexure. This flexure proved to be very sensitive to off center loadings and was difficult to calibrate. A four spoke flexure was manufactured and all four webs instrumented with strain gages to eliminate this deficiency. When the new flexure was installed, all the existing leads were used to obtain outputs from the four sets of strain gages installed on the webs. In order to obtain readouts from both the flexure and torque spool additional leads were required. However during the initial tests the torque on the closure plate was found to be less than one percent of the total torque on the stator assembly. Therefore, in the interest of saving time, new leads were not installed, and the strain gages on the torque spool were not connected during the final series of tests.

For data reduction purposes the torque on the closure plate was assumed to be constant, equal to 15 counts (0.276 ft.-lb.). The error in peripheral velocity caused by this assumption will be less than one-third of one percent.

Stator discharge pressure can be measured at the hub and tip radius only. The static pressure at the stator tip is measured by three equally spaced taps 0.25 in. downstream of the stator trailing edges. These taps are commoned to give an average tip static pressure.

The gap formed by the closure plate and the inner contour of the stator is 0.1275 in., and the outer edge of the closure plate is 0.020 in. inside of the inner flow passage of the stator discharge. The pressure existing in this gap

is assumed to be that at the hub of the stator. With the chamber formed by the bullet probe support, stator, and closure plate sealed from the atmosphere, the pressure in the gap is the pressure in the chamber.[6]

Tests were made at radial rotor tip clearances of 0.033 and 0.015 in. The larger clearance is obtained with the shroud of Fig. 5. This shroud has sixteen sets of three commoned static pressure taps, installed at 0.25 in. increments of the axial distance from the stator tip to the shroud exit. Additionally, one set of taps is arranged in the end face of the shroud.

For these tests the only pressures of interest were the stator tip static pressure and those that affect the axial force on the stator, namely, those measured by the two sets of taps on the bevel and the set on the end face of the shroud. With this shroud installed pressure and temperature surveys may be conducted at the rotor discharge.

A second shroud is available to permit surveys to be taken at the stator and rotor discharges, and in addition reduces the rotor radial tip clearance to 0.015 in. The pressure taps of this shroud are almost identical with those of the one previously described, with the difference that only two taps are arranged at each axial location. The second shroud has a double bevel at the exit instead of the single bevel shown in Fig. 5. Two sets of taps are installed in each bevel and at the end face of the shroud

---

[6]Vavra, M. H., Air Tests of the Mod I Ares Turbine, (Report Ares VA - T No. 8, 1966), p. 14.

to obtain a more accurate measurement of the pressures affecting the axial force on the stator.

All temperature probes are Iron-Constantan thermocouples. The cold junction is inserted in an ice bath to provide a 32^{o} F. reference. Temperatures are read, in millivolts, on a 48 channel Brown potentiometer.

All pressures are measured on a 96 in. high mercury manometer board with 0.1 in. graduations.

An accelerometer mounted on the bearing stand provides a means of monitoring the vibration patterns of the test rig. The output signal of the accelerometer is displayed on a Singer Panoramic Analyzer and on an RMS millivoltmeter.

All instrument readouts are located in the control room. Fig. 7 is a schematic representation of the instrumentation of the TTR for the evaluation of the performance of the Ares Mod II Turbine.

3. Test Procedures.

Evaluation of stator performance using the momentum and moment of momentum equations requires a high degree of accuracy in determining the axial forces that are exerted on the stator assembly. Therefore all force measuring devices must be carefully calibrated to insure the required degree of accuracy.

The force capsules measuring the net force and moment on the stator assembly are calibrated prior to each test run. A system of lever arms has been devised to apply torque and axial loads on the stator assembly with known weights.

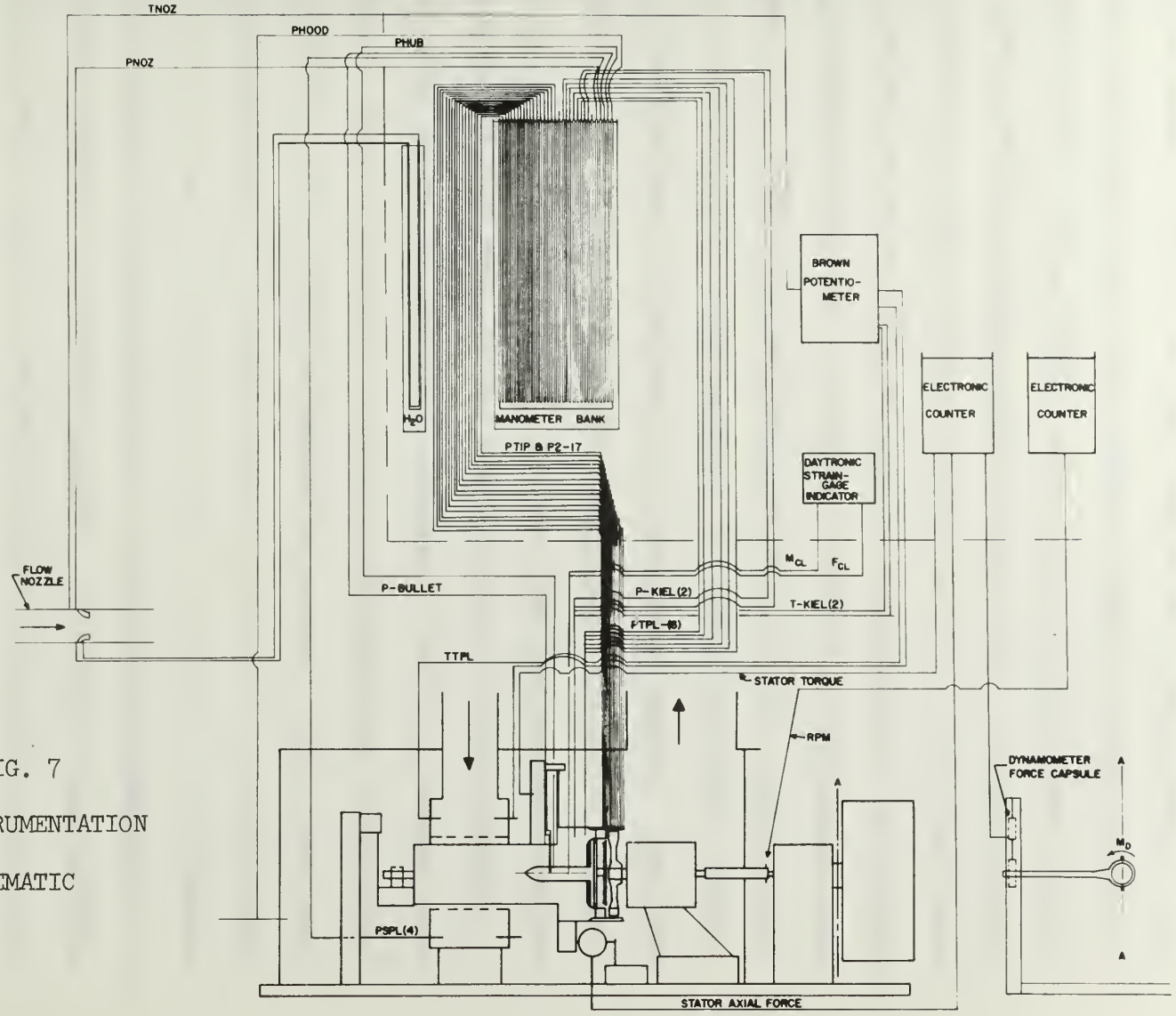

FIG. 7

TTR INSTRUMENTATION

SCHEMATIC

Axial force calibration is achieved by applying various axial loads on the stator assembly. The force capsule output is then linearized between ten and 12 KC. Linearization is accomplished by applying full load (160 lbs.) and adjusting the bandwidth to 12 KC, then removing the load to obtain a zero setting. Half load is then applied and the reading should be 11 KC. If the output is not 11 KC, the reading is changed in the direction of the error by an amount equal to three times the difference between 11 KC and the reading. Then the full and no load readings are readjusted to 12 and ten KC. This procedure is repeated until linearity is achieved. System hysteresis is checked by loading the assembly in 20 lb. increments from zero load to full load and then decreasing the load in like increments.

Stator torque is calibrated in the same manner as the axial force. In this instance, however, a torque load is obtained by applying the weights at the end of a 20 in. lever arm. Full load is attained with six 5 lb. weights resulting in a 50 ft.-lb. torque applied to the stator assembly.

Dynamometer calibration is performed with the dynamometer arm in position. This is taken as the zero load condition. The force capsule output is again linearized over a two KC range with the maximum reading corresponding to a dynamometer output of 800 in.-lb.

Initial tests were run with the dynamometer force capsule exposed, as shown in Fig. 4. During these tests a

great deal of difficulty was experienced in obtaining repeatable data. It was noted that, at the end of each test, the dynamometer output would not indicate zero load. Several attempts were made to determine the cause of this condition. It was finally ascertained that, even though the force capsule was said to be temperature insensitive in the test range, uneven heating or cooling caused large variations in the output signal. The source of the problem was exhaust from the dynamometer which discharges directly into the region where the capsule is mounted. Therefore, the force capsule was insulated from the dynamometer discharge air by installing an enclosure around it. To further insure that the capsule is maintained at a constant temperature, ambient air is blown through the enclosure by an electrically driven fan. This fan is situated outside the test cell to deliver air at almost constant temperature. The discharge of the fan is attached to a flexible tube of 3 in. diameter which is connected to the bottom of the enclosure.

After the dynamometer has been calibrated, its lever arm is lifted by hand to take a no-load tare reading of the force capsule. This tare provides a means of checking the capsule during the run for any long term temperature variation. The dynamometer arm is lifted periodically during the run and the reading obtained is compared with the tare reading. The dynamometer output is corrected by the difference of the two readings.

The axial force and torque on the closure plate can be calibrated only when the rotor is removed. However, these forces are measured by strain gages which do not require frequent calibration.

After the initial tests, it was found that the force capsules used to measure the axial force and torque on the stator assembly were affected in varying degrees by temperature changes also. However, these changes are not as radical as those experienced in the region of the dynamometer and may be easily compensated for. This is accomplished by noting the no load indication immediately after shutdown, and correcting the force and torque indication by an amount equal to the difference between the reading and the original calibration no-load reading. Since a relatively long temperature stabilization period is allowed prior to data acquisition, it is assumed that the force capsules reach temperature equilibrium also. During the initial test runs it was found that the torque on the closure plate was less than one percent of the net torque on the stator assembly. Additionally, the torque spool proved to be too rigid to achieve the desired sensitivity. Therefore, during the final tests, the closure plate torque was assumed to be constant.

Turbine Tests

During the test runs, periodic checks on the RPM measured by the electronic counter in the control room were made with a strobotac.

Thirty test runs were carried out at different pressure ratios, various axial clearances and radial clearances, over a range of speeds from 10,000 to 19,000 RPM. Mass flow rate variations at a given pressure ratio were achieved by operating with or without the exhauster assembly.

Runs 51 through 63 were made at a radial clearance of 0.033 in. and axial clearances of 0.2, 0.41, 0.64, 1.0 and 1.5 inches. Pressure ratios of 1.3, 1.4, 1.5, and 1.6 were chosen for the test operating conditions with the exhauster installed. These pressure ratios gave the widest range of data within the design regime of the Mod II turbine. When operating without the exhauster, pressure ratios of 1.3, 1.4, and 1.5 were chosen with only a limited operating range available at 1.5.

The pressure ratio across the turbine is controlled by two factors, namely, the vacuum produced in the hood by the exhauster, and the total pressure at the turbine inlet. For a high vacuum and a low inlet pressure, the mass flow rate through the turbine at a particular pressure ratio is smaller than that which occurs at a low vacuum and high inlet pressure, since the turbine flow rate is nearly proportional to the turbine inlet pressure.

If the inlet valve to the first settling tank is fully open, the total airflow through the turbine and the exhauster is regulated by the compressor discharge valve which controls the amount of compressor air delivered to the first settling tank of Fig. 1. The distribution of supply

air to the two components is controlled by an electrically operated exhauster inlet valve and a manually operated turbine inlet valve. Movement of either of these two valves alters the flow rate through both the exhauster and the TTR. An increase in airflow through the exhauster is accompanied by a decrease in flow through the turbine, and vice versa.

It was found that the most satisfactory results were obtained by leaving the exhauster inlet valve completely open at all times. With the exhauster inlet valve only partially open, large oscillations from the mean were noted in the pressure at the flow nozzle which resulted in flow instabilities throughout the TTR. If this valve is fully open, the pressure ratio across the turbine can be controlled by the turbine inlet valve and the compressor discharge valve.

To obtain the best possible data correlation, the turbine inlet conditions were set at chosen fixed values for each pressure ratio. These settings were used each time for a given pressure ratio. By operating in this manner any deviations from the norm could be easily recognized and corrected.

The rotor axial clearance was adjusted prior to each test run by moving the bearing housing in the rotor bearing stand. After adjusting the axial clearance, the dynamometer bearing housing is positioned to insure that the shaft splines of the rotor and dynamometer are engaged with the splines of the quill shaft over their whole axial length.

Just prior to commencing a test run, the two valves controlling the oil flow to the oil-mist producer for the rotor and dynamometer bearings and the air supply valve are turned on.

For a test run, the various control valves are set as follows:

1. Exhauster inlet - fully open
2. Turbine inlet - partially open
3. Compressor discharge - fully open
4. Inlet to the first settling tank - closed.

After the Allis-Chalmers compressor has been operating for a sufficient length of time to provide for temperature stabilization, the turbine is brought up to speed by opening the inlet valve to the first settling tank. When this valve is fully opened, the desired flow conditions are obtained by adjusting the compressor discharge and turbine inlet valves. At the beginning of each run the air dynamometer is usually set for maximum power absorption, to give minimum turbine speed. Once the desired flow conditions have been obtained, temperatures throughout the test installation must be allowed to stabilize prior to taking data.

The general procedures for taking data were as follows:

1. The pressure at the flow nozzle is recorded.

2. The following items may be recorded in any order, but must be taken when the nozzle pressure is at the point recorded in 1.

a. Pressure drop across the flow nozzle.

b. RPM

c. Dynamometer torque

d. Stator torque

e. Stator axial force

f. Closure plate axial force

g. Closure plate torque

h. Shroud pressures

i. Total plenum pressures

j. Static plenum pressure

k. Hub pressure

l. Hood pressure.

3. The following temperatures are recorded:

a. Temperature ahead of the flow nozzle

b. Total plenum temperatures (2)

c. Bullet probe temperature

d. Kiel temperatures (2)

4. The dynamometer arm is lifted and a no-load tare reading is recorded.

5. The dynamometer load absorption is reduced and steps (1) through (4) are repeated for the higher speed. Usually eight data points were recorded at each pressure ratio. If more than one pressure ratio was investigated during a run, the desired ratio was set and steps (1) through (5) were repeated.

This data taking procedure was not used during all tests. After the results of the first runs were studied, various

procedures were tried out to produce more repeatable results. In general it was recognized that, without the temperatures being stabilized, significant variations occurred while recording the data. However, if the temperatures were allowed to stabilize, they would remain constant while recording the remainder of the data. It should be noted here that whenever the mass flow rate through the turbine is altered significantly, by changing the turbine pressure ratio, the temperatures must again be allowed to reach a new steady state.

It was also noted that small changes in the pressure level ahead of the flow nozzle affected the RPM, the dynamometer reading, and the force capsule readouts almost instantaneously. However, total pressure at the turbine inlet, observed on the manometer board, lagged significantly behind the above mentioned readouts.

It is therefore necessary to set a definite value for the pressure at the flow nozzle inlet and to record the data only if this pressure can be maintained. Only with this procedure will it be possible to obtain test points for the proper flow rate.

The total pressure at the stator inlet varies somewhat if the RPM is changed. Therefore it is necessary to readjust this pressure to maintain a desired pressure ratio.

Pressure, temperature, and velocity surveys were conducted at the stator and rotor discharge during runs 64, 65, 66, 67, 74, 75, 76, and 79. For these surveys, the

exhauster assembly and the hood were removed. Prior to these tests the second rotor shroud was installed which has a radial rotor tip clearance of 0.015 in. Operation of the TTR without the exhauster is essentially the same as previously described. Then the exhauster inlet valve is closed, the turbine inlet valve is fully open, and the rotor discharges directly into the atmosphere. Thus the total pressure at the stator inlet is completely controlled by the compressor discharge valve.

The surveys were made with a United Sensor DA-125 five hole probe. With this probe it is possible to determine the pitch angle, yaw angle, total pressure, and dynamic head at the stator and rotor discharge. Fig. 8 is a picture of the probe and its supporting bracket as installed in the TTR.

An additional survey was made at the stator inlet with one of the two movable Kiel probes to obtain total pressure variations at various radial positions of the probe.

The surveys at the stator and rotor discharge give an indication of the flow discharge angles, pitch angles, and absolute velocities at these locations.

The total pressure tap (#1), and one of the two static pressure taps (#2) or (#3) of the probe of Fig. 8, were connected to either side of a mercury manometer. Additionally, the total pressure tap was connected to one side of a mercury manometer with the other side open to the atmosphere. The two static pressure taps, (#2) and (#3), and

TABLE I

MOD II TURBINE TEST RUNS 1967

Jan.-Aug.

Run No.	r (in.)	X (in.)	$\frac{P_{t_o}}{P_2}$	N (RPM)	Test Purpose
			(approx.)	**Varied	+ = Performance Characteristics
○ 51	0.033	0.410	1.4, 1.5	**13-20,000	+
* 52		0.620	1.4, 1.5	14,000	Test Hood Checkout
* 53		0.620	1.3, 1.4 1.5	**11-18,000	+
* 54		0.410	1.6, 1.8	**15-18,000	+
○ 55		0.410	-	0	Dynamometer Calibration
* 56		0.410	1.4	**13-19,000	" "
* 57		0.410	1.4	**13-19,000	Spring Capsule Check
* 58		0.620	1.3, 1.5 1.6	**10-17,000	+
* 59		1.000	1.3, 1.4, 1.5, 1.6	**10-17,000	+
* 60		0.200	1.3, 1.4 1.5, 1.6	**10-17,000	+
* 61		0.410	1.3, 1.4	**11-17,000	+
* 62		0.410	1.5, 1.6	**13-17,000	+
* 63		1.500	1.3, 1.4 1.45, 1.5, 1.6	**11-19,000	+
○ 64	0.015	1.000	1.4	14,600	Stator Exit Survey
○ 65			1.4	14,600	" " "
○ 66			1.4	14,600	" " "
○ 67			1.4	14,600	Rotor Exit Survey
* 68			1.3, 1.4 1.5, 1.6	**11-18,000	+
* 69		0.410	1.3, 1.4 1.5	**11-19,000	+

TABLE I (CONT'D)

MOD II TURBINE TEST RUNS 1967

Jan.-Aug.

Run No.	r (in.)	x (in.)	$\frac{P_{t_o}}{P_2}$	N (RPM)	Test Purpose
			(approx.)	**Varied	+ = Performance Characteristics
*70	0.015	0.410	1.6	**14-19,000	+
*71		0.200	1.3, 1.4	**11-17,000	+
*72		0.410	1.3, 1.4 1.5	**11-18,000	Repeat Run 69
*73		0.200	1.3, 1.5		Repeat Run 71
°74		0.200	1.3, 1.4		Repeat Run 71
°75		0.410	1.3	11,500	Stator Entrance & Exit Survey
°76		0.410	1.3, 1.4 1.5	**11,400-19,000	Rotor Exit Survey
°77		0.410 & 1.000	1.3, 1.4	**11,400-19,000	+
°78		.200, .410, 1.000	1.3	**11,400-18,000	Spring Capsule Check
°79		.200	1.3, 1.4	**11-17,000	Repeat Run 71
°80		.410	1.3	Varied	

* With Exhauster $p_2 < p_{barometer}$

° Without Exhauster $p_2 = p_{barometer}$

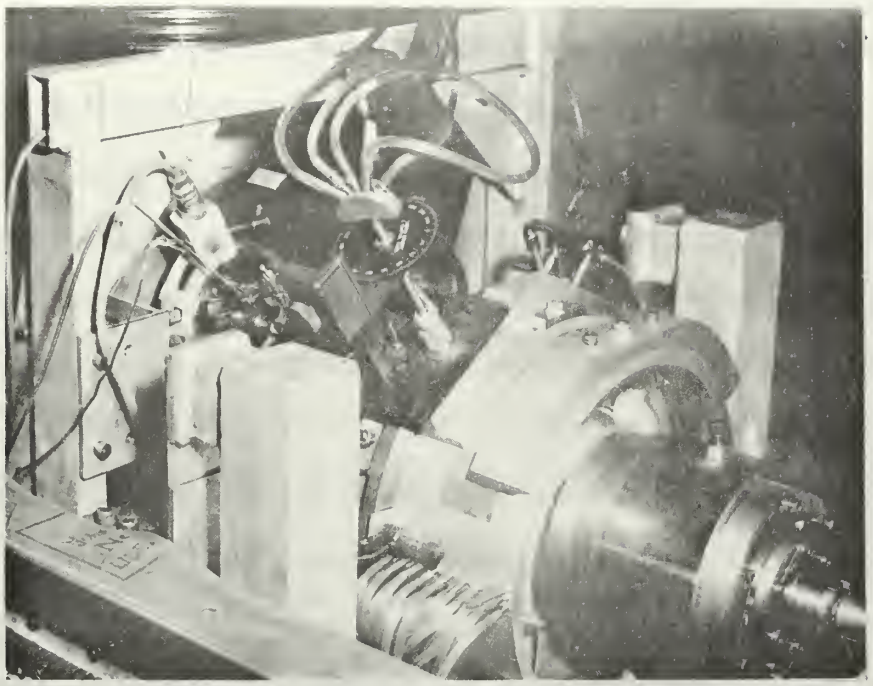

(a)

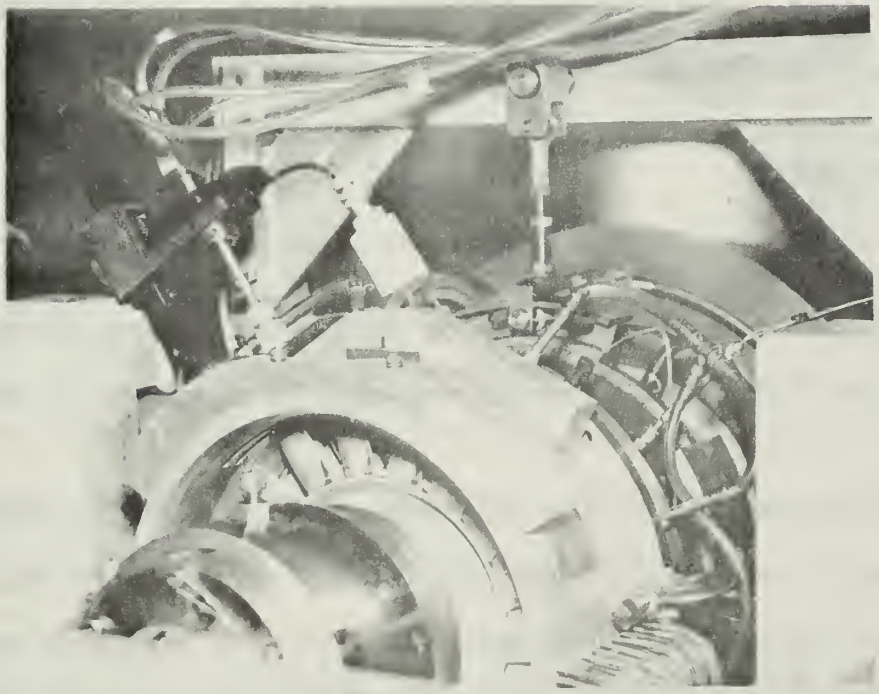

(b)

FIG. 8

TRAVERSE PROBE INSTALLATION

(a) View showing Protractor. (b) View showing probe in blade passage.

the taps used to measure pitch angle, (#4) and (#5), were each connected to either side of a water manometer.

During the tests the probe was first turned about its axis until the pressures indicated by taps (#2) and (#3) were balanced to establish the flow direction. The flow angle is then read from a protractor attached to the probe, which is adjusted to read zero when the probe is aligned with the axis of the turbine.

Temperature surveys were also made at the stator and rotor discharge with a Kiel probe mounted in the same manner as the pressure probe.

Table I is a list of the runs performed, showing the radial and axial clearances, pressure ratios, speed ranges and test purpose for each run.

4. Data Reduction.

General

The method of analysis used to evaluate turbine performance is a one dimensional, mean streamline approach given by Vavra.[7]

The equations of continuity, momentum, moment of momentum and energy are used in the analysis. Of primary concern here is the use of the momentum and moment of momentum equations to accurately predict the flow conditions at the stator discharge. However, given in the following is also a

---

[7] Vavra, M. H., Aero-Thermodynamics and Flow in Turbomachines (New York, London: John Wiley and Sons, Inc., 1960) Chap. 15

complete description of the data reduction methods employed to obtain the overall turbine performance.

A program (TTR2) was written to reduce the data on the IBM 360 Computer of the Naval Postgraduate School. A program description and a sample program are given in Appendix A.

Flow Rate Determination

The turbine flow rate is equal to the flow through the flow nozzle less the plenum labyrinth seal leakage flow

$$\dot{w}_t = \dot{w}_n - \dot{w}_l \qquad (1)$$

The nozzle flow rate is obtained from the basic flow equation for a flow nozzle:[8]

$$\dot{w}_n = 359.1\, D_n^2\, \alpha_n\, C_n\, Y_1 \sqrt{\rho_1 h_w} \quad \text{(lbm/hr)}$$

where

D_n = nozzle throat diameter (in.)

α_n = coefficient of thermal expansion (dimensionless) based on D_n^2

C_n = discharge coefficient (dimensionless)

Y_1 = expansion coefficient (dimensionless)

ρ_1 = fluid density at the upstream tap (lbm/ft^3)

h_w = differential pressure across taps (in. H_2O)

For the flow nozzle, made of 2024-T4 aluminum:[9]

$$\alpha_n = 1 + 0.00252 \left(\frac{T_{noz} - 527.7}{100}\right)$$

---

[8] Stearnes, R. F., et. al., Flow Measurement with Orifice Meters (New York: Van Nostrand Co., Inc., 1951), p. 6.

[9] Eckert, R. H., Performance Analysis and Initial Tests of a Transonic Turbine Test Rig (Naval Postgraduate School, 1966), p. 99.

The nozzle discharge coefficient, C_n, was first determined by Eckert and then by Naviaux. Naviaux shows that the nozzle discharge coefficient is constant, equal to 1.05, above a Reynolds Number of 9.75×10^5.[10]

All tests were performed at mass flow rates corresponding to Reynolds Numbers in the region where C_n is a constant.

The expansion coefficient for a flow nozzle is

$$Y_1 = \left[\frac{\gamma}{\gamma - 1} \frac{\left(P_2/P_{noz}\right)^{2/\gamma} - \left(P_2/P_{noz}\right)^{\gamma+1/\gamma}}{1 - \left(P_2/P_{noz}\right)} \frac{1 - \beta^4}{1 - \beta^4 \left(P_2/P_{noz}\right)^{2/\gamma}} \right]$$

where β is the diameter ratio D_n/D_1.[11] The final form of the basic flow equation with all pressures in pounds per square inch, and temperatures in degrees Rankine, becomes:

$$\dot{w}_n = 0.8633 \, D_n^2 \propto_n C_n \, Y_1 \sqrt{\frac{P_{noz} \, h_w}{T_{noz}}}$$

The leakage flow rate through the plenum labyrinths has been obtained from tests.[12]

$$\dot{w}_1 = 0.116 \frac{\phi_1 P_{sp1}}{\sqrt{T_{tp1}}}$$

---

[10] Naviaux, J. C., Transonic Turbine Test Rig Exhauster System Tests and Tests of a Reaction Turbine (Naval Postgraduate School, 1966), p. 68.

[11] Asme Power Test Codes, Information on Instruments and Apparatus, Part 5, Chapter 4, Flow Measurement by Means of Standard Nozzles and Orifice Plates.

[12] Eckert, R. H., Performance Analysis and Initial Tests of a Transonic Turbine Test Rig (Naval Postgraduate School), 1966), p. 113.

where

$$\Phi_1 = \sqrt{\frac{1 - P_{hood}/P_{SP1}}{4.0791}}$$

Then the turbine mass flow rate is found from Eq. (1).

Stator Analysis

To obtain the stator performance characteristics by the application of the momentum, and the moment of momentum equations, requires a high degree of accuracy in the measurement of the pressures and forces acting on the stator assembly. Since the force on the stator assembly is small, any error in the pressure readings manifests itself in a relatively large error in the net force which is used to determine the axial velocity. This is especially true for pressures at the hub and tip of the stator since they are multiplied by relatively large areas.

To evaluate the general momentum theorem as given by Vavra,[13]

$$\frac{\partial}{\partial t}\left[\int_R dm_s \bar{V}\right] + \int_{S_1} dm_s \bar{V}_1 - \int_{S_o} dm_s \bar{V}_o = \int_S -\bar{n} p \, dS + \int_S -\bar{t} \tau \, dS + \bar{G} \tag{2}$$

and to apply the results to determine stator performance, certain simplifying assumptions will be made; namely:

---

[13] Vavra, M. H., Aero-Thermodynamics and Flow in Turbomachines (New York, London: John Wiley and Sons, Inc., 1960), Chap. 5.

1. The flow is steady and adiabatic.

2. The flow is axisymmetric with no initial peripheral component and no radial component throughout.

3. The operating fluid is a perfect gas with a constant specific heat.

4. Shear stresses on the inner perimeter of the shroud and at the discharge annulus are ignored. The integral of the latter is small.

Since the test rig is designed so that the airflow enters the floating stator assembly without an axial component, Eq. (2) may now be reduced to

$$\int_{S_1} dm_s \bar{V}_1 = \int_S -\bar{n} p \, dS \qquad (2a)$$

where the term representing the weight of the fluid particles in the control region has been ignored since it is small in relation to the inertia forces. For the control region shown in Fig. 9, the terms on the right hand side of Eq. (2a) become

$$\int_S -\bar{n} p \, dS = \int_{A_2} -\bar{n} p_{17} \, dA + \int_{A_3} -\bar{n} \frac{(p_{14} + p_{15} + p_{16})}{3} dA$$

$$+ \int_{A_4} -\bar{n} p_{TIP} \, dA + \int_{A_5} -\bar{n} p_1 \, dA + \int_{A_6} -\bar{n} p_{hub} \, dA$$

$$+ \int_{A_1} +\bar{n} p_{hood} \, dA + \int_{S_w} -\bar{n}_w p_w \, dS_w + \int_{A_7} -\bar{n} (p_7 - p_{hub}) dA$$

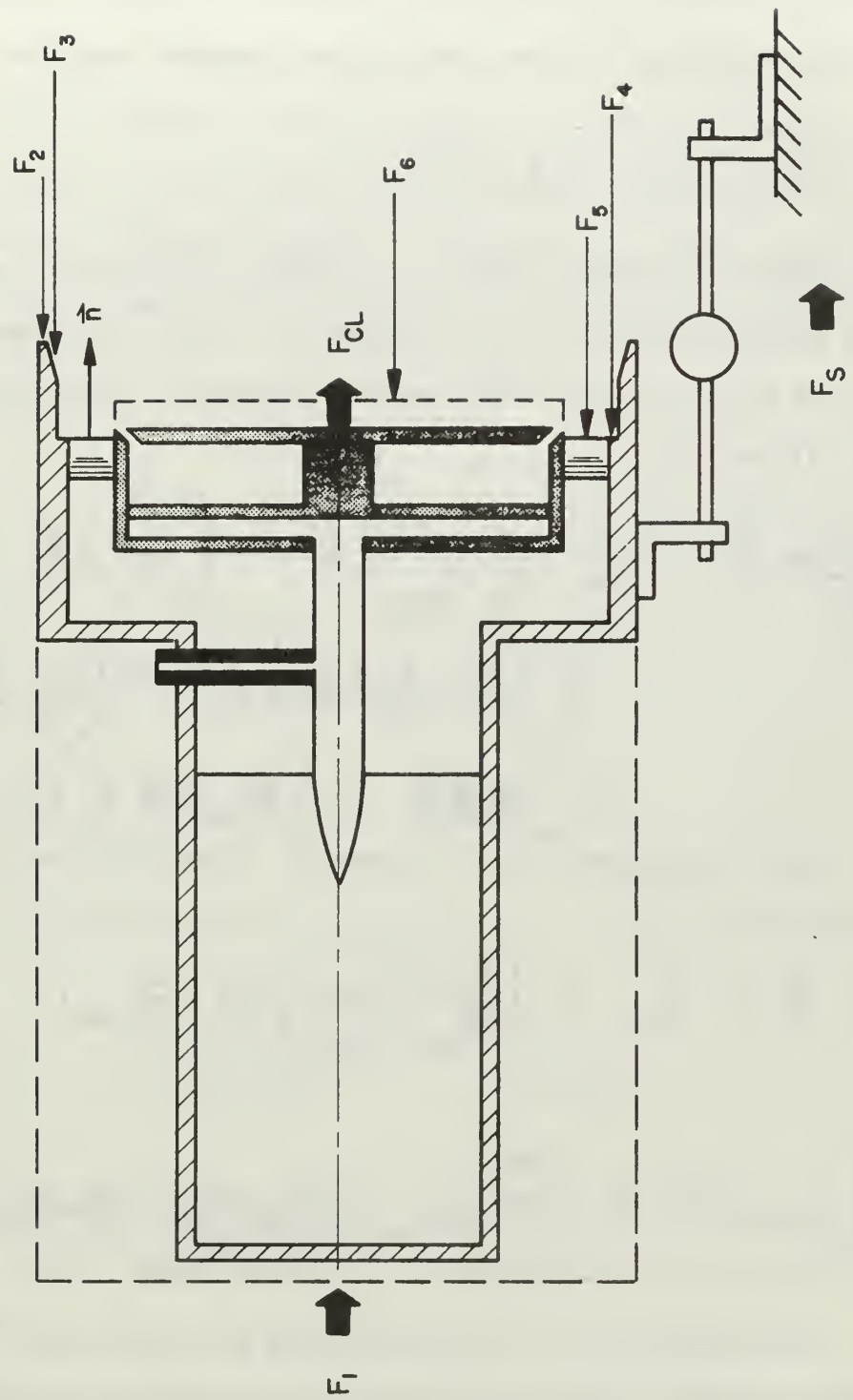

SCHEMATIC OF STATOR FORCES
FIG. 9

The last integral on the right-hand side of Eq. (3) is the measured force exerted on the closure plate, F_{cl}. The seventh integral is the force exerted by all the surfaces in contact with the flow inside the control region.

$$\bar{F}_s = \int_{S_w} -\bar{n}_w p_w \, dS_w$$

The component of this term in the axial direction is the force measured by the force capsule. Since the remaining terms of Eq. (3) have only axial components, combining Eqs. (2) and (3)

$$\int_{A_5} dm_s V_{a_1} = F_s + \int_{A_1} p_{hood} \, dA - \int_{A_2} p_{17} \, dA - \int_{A_3} \left(\frac{p_{14} + p_{15} + p_{16}}{3} \right) dA - \int_{A_4} p_{tip} \, dA - \int_{A_5} p_1 \, dA - \int_{A_6} p_{hub} \, dA + F_{cl} \tag{4}$$

for an assumed linear pressure distribution from stator hub to tip

$$p_1 = p_{hub} + \left(\frac{p_{TIP} - p_{hub}}{R_{tip_1} - R_{hub_1}} \right) (R - R_{hub_1})$$

then

$$\int_{A5} p_1 \, dA = \int_{R_{hub_1}}^{R_{TIP_1}} 2\pi \left[p_{hub} + \left(\frac{p_{tip} - p_{hub}}{R_{tip_1} - R_{hub_1}} \right) (R - R_{hub_1}) \right] R \, dR \tag{4a}$$

The remainder of the pressures are measured, and forces caused by them are simply the pressures times their respective areas. Solving Eq. (4) for V_{a_1}

$$V_{a_1} = \frac{\int dm_s V_{a_1}}{m_s} = \frac{g}{\dot{w}_t}\left[F_s + F_{c_1} + F_1 - \sum_{i=2}^{6} F_i\right] \qquad (5)$$

where F_i are the pressure forces, and $m_s = \dot{w}_t/g$.

The peripheral component of the stator discharge velocity is obtained by applying the moment of momentum equation to the control region. Applying the same simplifying assumptions used in the previous development for determining V_{a_1}

$$M = \int_{s_o} dm_s R_o V_{u_o} - \int_{s_1} dm_s R_1 V_{u_1}$$

Since the flow enters the stator axially, $V_{u_o} = 0$, and ignoring algebraic signs,

$$M = \int_{s_1} dm_s R_1 V_{u_1} \qquad (6)$$

With the mean streamline approach

$$V_{u_1} = \frac{\int_{s_1} dm_s R_1 V_{u_1}}{m_s R_{m_1}} = \frac{M}{m_s R_{m_1}} \qquad (7)$$

The moment measured by the force capsule is not equal to M. There is an additional moment imparted to the closure plate due to the shear forces in the peripheral direction. These forces are the result of the rotating motion imparted to the fluid by the turbine wheel. There also exists a moment on the inner face of the shroud caused by

shear forces in the peripheral direction. However, for this analysis this latter moment was ignored and the net moment created by the change in peripheral velocity is taken as

$$M = (M_s + M_{cl}) \tag{8}$$

where M_{cl} is the moment caused by shear forces on the closure plate, and M_s is the measured moment on the stator assembly. Then, combining Eqs. (7) and (8)

$$V_{u_1} = \frac{g(M_s + M_{cl})}{R_{m_1} \dot{w}_t} \tag{9}$$

where

$$R_{m_1} = \sqrt{\frac{R_{tip1}^2 + R_{hub1}^2}{2}}$$

Using the results obtained from Eqs. (5) and (9)

$$V_1 = \sqrt{V_{u_1}^2 + V_{a_1}^2} \tag{10}$$

and the absolute discharge angle

$$\alpha_1 = \tan^{-1}\left(V_{u_1}/V_{a_1}\right)$$

Since the flow is assumed to be steady and adiabatic, and because there is no work done in the stator, the total enthalpy along the mean streamline must remain constant. Therefore,

$$H = h_1 + \frac{V_1^2}{2gJ} \tag{11}$$

With the perfect gas assumption, Eq. (11) reduces to

$$T_{tp1} = T_1 + \frac{V_1^2}{2gJc_p}$$

Solving for T_1,

$$T_1 = T_{tp1} - \frac{V_1^2}{2gJc_p} \tag{12}$$

For an isentropic process

$$T_{1_{is}} = T_{tp1}\left(\frac{p_1}{p_{tp1}}\right)^{\frac{\gamma-1}{\gamma}} \tag{13}$$

Thus, the stator loss coefficient is defined by

$$\zeta_s = \frac{T_1 - T_{1_{is}}}{\Delta T_{is}} = \frac{T_1 - T_{1_{is}}}{T_{tp1} - T_{1_{is}}} \tag{14}$$

and the stator efficiency is

$$\eta_s = 1 - \zeta_s$$

To insure that the solution obtained from momentum satisfies continuity as well, a check is performed by utilizing flow functions defined by Vavra.[14]

$$\Phi = \frac{\dot{W}_t}{p_{tp1} A_{th}}\sqrt{T_{tp1}\frac{R}{g}} = \left[\frac{2\gamma}{\gamma-1}\left(\left(\frac{p_{th}}{p_{tp1}}\right)^{2/n} - \left(\frac{p_{th}}{p_{tp1}}\right)^{\frac{n+1}{n}}\right)\right]^{1/2} \tag{15}$$

where

$$n = \frac{\gamma}{1 + \zeta_p(\gamma-1)} \tag{16}$$

and

$$A_{th} = a\bar{Z}h$$

---

[14] Vavra, M. H., Problems of Fluid Mechanics in Radial Turbomachines (Rhode-Saint Genese, Belgium, Von Karman Institute of Fluid Dynamics, 1965), VKI Course Note 55a Equation C (7).

Φ represents a non-dimensional flow rate. The right hand side of Eq. (15) is a function of pressure ratio, the value of γ, and the polytropic loss coefficient ζ_p. The pressure at the throat is not a measured quantity. For want of a better understanding of the phenomena involved, it will be assumed that throat pressure and discharge pressure are equal. Fig. 10 shows the stator flow passage.

With the assumption that the static pressure at the throat equals that after the stator

$$\Phi = \left[\frac{2\gamma}{\gamma-1} \left(\left(\frac{p_1}{p_{tp1}} \right)^{2/n} - \left(\frac{p_1}{p_{tp1}} \right)^{n+1/n} \right) \right]^{1/2}$$

Fig. 11 represents an adiabatic expansion process with friction in a channel with varying cross sections. The derivation of the polytropic loss coefficient is given by Vavra[15]

$$dT_{is} = T\left[1 - \left(\frac{p - dp}{p} \right)^{\frac{\gamma-1}{\gamma}} \right] = T\left[\frac{\gamma-1}{\gamma} \frac{dp}{p} \right] \quad (17)$$

letting

$$1 - \zeta_p = \frac{dT}{dT_{is}} \quad (18)$$

ζ_p is assumed to be constant throughout the expansion process. Combining Eqs. (17) and (18)

$$\frac{dT}{T} = \left(1 - \zeta_p \right) \left(\frac{\gamma-1}{\gamma} \frac{dp}{p} \right) \quad (19)$$

---

[15] Ibid., p. C23.

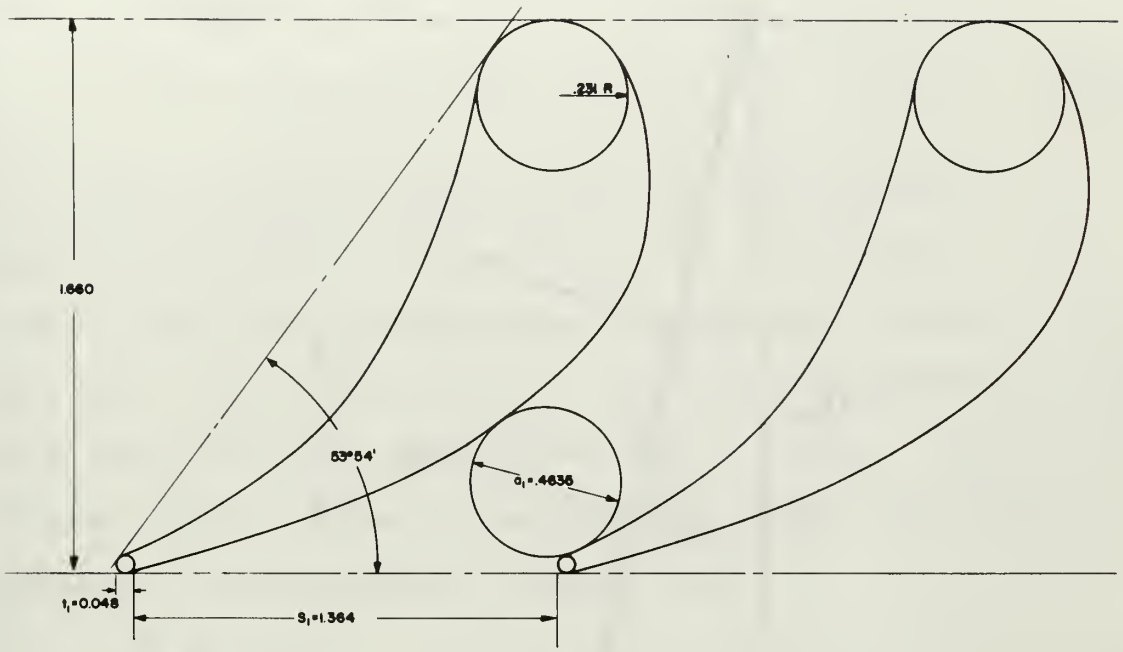

FIG. 10

STATOR BLADE PROFILE

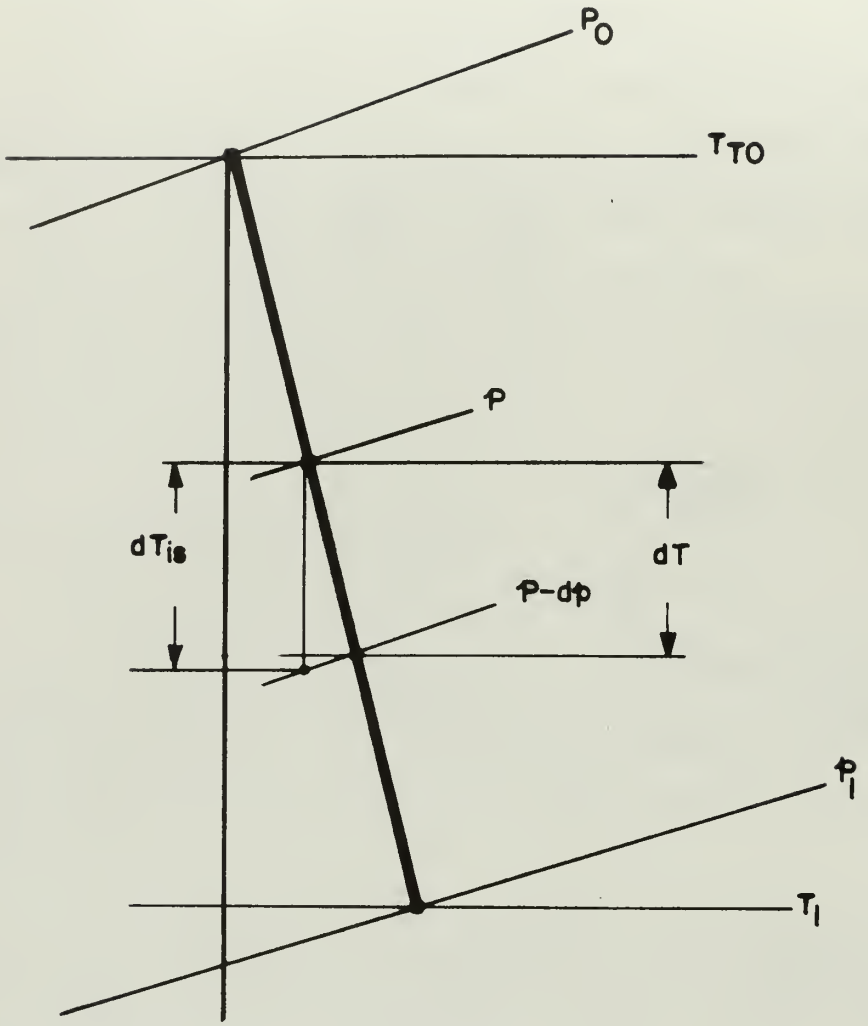

FIG. 11

EXPANSION PROCESS WITH FRICTION

Integrating Eq. (19)

$$T = (\text{constant})\ p^{(1-\zeta_p)\frac{\gamma-1}{\gamma}} \tag{20}$$

Eq. (20) may be expressed as

$$T = (\text{constant})\ p^{\frac{n-1}{n}} \tag{21}$$

The expression shown in Eq. (16) is obtained by setting the exponents of Eq. (20) and Eq. (21) equal to each other. The actual stator loss coefficient is defined by Eq. (14). The polytroic loss coefficient is somewhat higher than the actual loss coefficient due to reheat. However, at low pressure ratios the difference is less than three percent. It is therefore assumed that

$$\zeta_p = \zeta_s \tag{22}$$

With this assumption Eq. (16) becomes

$$n' = \frac{\gamma}{1 + \zeta_s(\gamma-1)} \tag{23}$$

The three percent error introduced by Eq. (22) manifests itself in a change of less than one tenth of a percent in the polytropic exponent shown in Eq. (23).

Using the value of the polytropic exponent from Eq. (23) in Eq. (15)

$$\frac{\dot{W}_t}{T_{tpl} A_{th}} \sqrt{T_{tpl} \frac{R}{g}} = \left[\frac{2\gamma}{\gamma-1} \left(\left(\frac{P_1}{P_{tpl}} \right)^{\frac{2}{n'}} - \left(\frac{P_1}{P_{tpl}} \right)^{\frac{n'+1}{n'}} \right) \right]^{1/2} \tag{24}$$

The quantities on the left-hand side of Eq. (24) are either known or measured quantities; therefore, it is assumed

to be correct. P_1, however, is not measured but is based on the assumption that the pressure distribution at the stator discharge is linear. If this assumption is incorrect, Eq. (24) will not be satisfied. Therefore an iterative process is adopted in which p_1 is changed until Eq. (24) is satisfied. Each time p_1 is incremented, V_{a_1} is recomputed using Eq. (5). Since V_{u_1} is unaffected by changes in p_1, its value will remain constant. The quantities V_1, T_1, and $T_{1_{is}}$ are recomputed to obtain a new stator loss coefficient, which is then used to obtain a new value for the polytropic exponent which is introduced into Eq. (24) for a subsequent check. This process is repeated until Eq. (24) is satisfied. The solution finally obtained will satisfy both momentum and continuity within the limits of the adopted assumptions.

The isentropic flow function is defined by

$$\Phi_{is} = \left[\frac{2\gamma}{\gamma-1}\left(\left(\frac{p_1}{p_{tp1}}\right)^{\frac{2}{\gamma}} - \left(\frac{p_1}{p_{tp1}}\right)^{\frac{\gamma+1}{\gamma}}\right)\right]^{1/2} \tag{25}$$

This flow function holds for an isentropic expansion process from P_{tp1} to p_1.

If the expansion process were isentropic, the area required to pass the flow would be less than that for the same process with friction. The area blockage factor is defined as

$$\xi = \frac{\Phi}{\Phi_{is}} \tag{26}$$

ξ represents the percentage of the throat area that would be required to pass the flow if the expansion were isentropic.

Rotor Analysis

The analysis of the rotor performance is based on the moment of momentum equation. For this application the moment of momentum equation is

$$M = \int_{S_1} dm_s \, R_1 \, V_{u_1} - \int_{S_2} dm_s \, R_2 \, V_{u_2} \tag{27}$$

The moment shown in Eq. (27) represents the moment exerted on the rotor by the fluid due to the change in peripheral velocity across the rotor, which is measured by the dynamometer.

The first integral on the right-hand side of Eq. (27) was evaluated in the previous section. Combining Eq. (7) with Eq. (27)

$$\int_{S_2} dm_s \, R_2 \, V_{u_2} = m_s \, R_{m_1} \, V_{u_1} - M_D \tag{28}$$

Again assuming that the average peripheral component acts at the mean streamline

$$V_{u_2} \, R_{m_2} \, m_s = \int_{S_2} dm_s \, R_2 \, V_{u_2} \tag{29}$$

Substituting Eq. (29) for the left hand side of Eq. (28) and solving for V_{u_2}

$$V_{u_2} = \frac{R_{m_1}}{R_{m_2}} \, V_{u_2} - \frac{M_D g}{\dot{w}_T \, R_{m_2}} \tag{30}$$

where $\dot{w}_t/g = m_s$.

The rotor analysis is greatly simplified by introducing the so-called equivalent total enthalpy and total pressure as defined by Vavra.[16]

The state point shown at E in Fig. 12 is defined by H_E and P_{t_E}. By defining a state point in this manner the expansion process through the rotor may be evaluated as if the flow passage were a stationary blade row. The equivalent total enthalpy is obtained from

$$H_E = h_1 + \frac{W_1^2}{2gJ} - \left(\frac{U_1^2 - U_2^2}{2gJ}\right) \tag{31}$$

where W_1 is the relative velocity of the flow at the rotor entrance. Its relationship to the absolute velocities at the stator discharge is shown in Fig. 13. With the known quantities V_1, U_1, and α_1, W_1 may be found from

$$W_{a_1} = V_{a_1}$$

$$W_{u_1} = V_{u_1} - V_1$$

and

$$\beta_1 = \tan^{-1} \frac{W_{u_1}}{W_{a_1}}$$

Then

$$W_1 = \sqrt{W_{u_1}^2 + W_{a_1}^2}$$

The equivalent total enthalpy and temperature are established once the conditions at the stator discharge are known. However, the state point E cannot be immediately

---

[16] Ibid., p. G4.

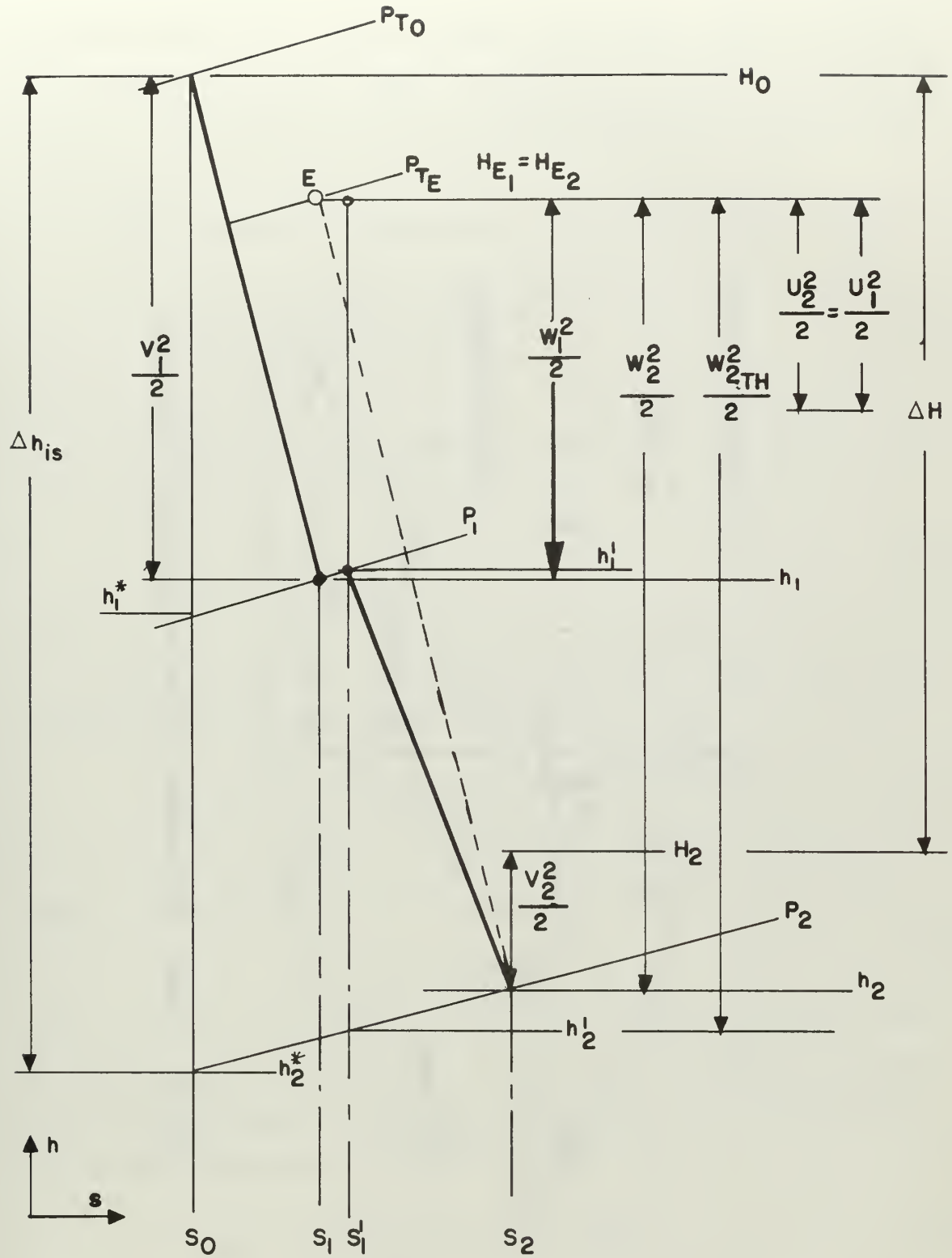

FIG.12 THERMODYNAMIC PROCESS OF FLUID IN TURBINE STAGE

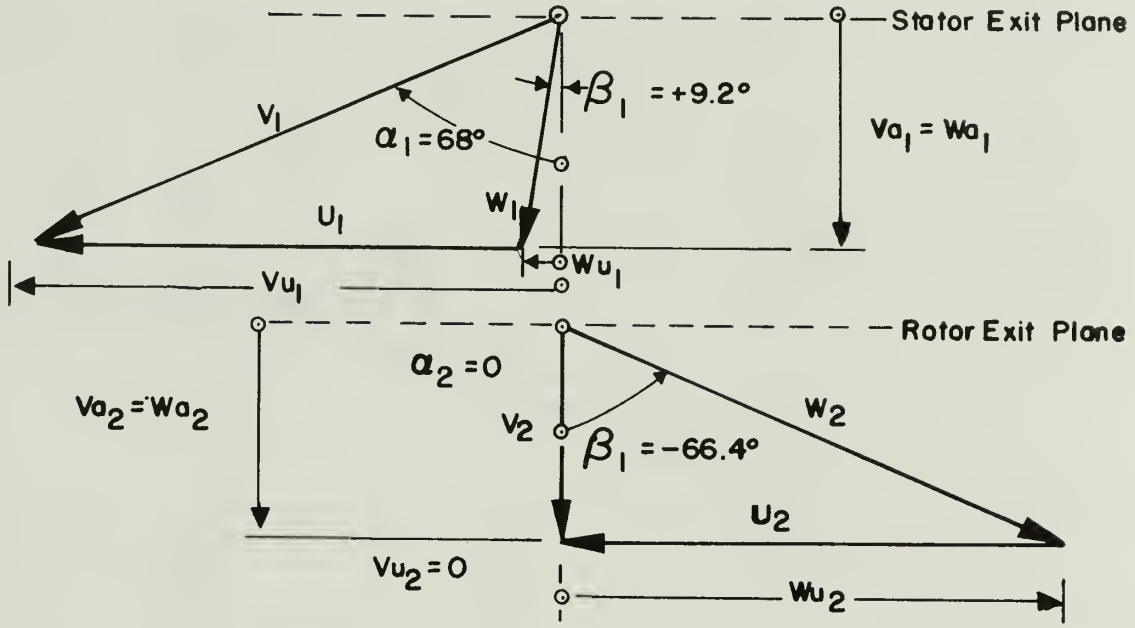

FIG. 13 MEAN STREAMLINE, DESIGN POINT, VELOCITY DIAGRAM

defined unless the losses between the blade rows are known. The conditions at the rotor discharge may still be obtained. However, the complexity of the calculations is somewhat increased.

The isentropic temperature change from T_{t_E} to $T_{2_{is}}$ is

$$\Delta T_{is} = T_{t_E}\left[1 - \left(\frac{P_2}{P_{t_E}}\right)^{\frac{\gamma-1}{\gamma}}\right] \tag{32}$$

It is assumed that p_2 is equal to the hood pressure or ambient pressure when operating without the exhauster. Then the rotor efficiency is obtained from

$$\eta_r = \frac{T_{t_E} - T_2}{\Delta T_{is}} \tag{33}$$

Solving Eq. (33) for T_2 and substituting for ΔT_{is} from Eq. (32) the resulting expression is

$$T_2 = T_{t_E}\left\{1 - \eta_r\left[1 - \left(\frac{P_2}{P_{t_E}}\right)^{\frac{\gamma-1}{\gamma}}\right]\right\} \tag{34}$$

Applying continuity at the rotor discharge

$$\dot{w}_t = \rho_2 W_{a_2} (A_2 k_{t_r}) \tag{35}$$

where A_2 is the annulus area at the rotor discharge and k_t is a restriction factor to account for the blade trailing edge thickness. The relationship for k_t, developed from data presented by Beer,[17] is

$$K_t = 1 - \frac{2.7}{10^3}\left(\frac{t}{s}\,100\right)^{3.3}\frac{a}{s} \tag{36}$$

---

[17] Beer, R., Aerodynamic Design and Estimated Performance of a Two Stage Curtis Turbine for the Liquid Oxygen Turbopump of the M-1 Engine (NASA CR 54764 A6 C8800-12, 1965), Fig. 20.

where

t = the blade trailing edge thickness

S = blade spacing

a = throat dimension

Eq. (36) is not directly applicable to a rotating blade row due to the increase in flow area resulting from tip clearance. The increased area reduces the effect of area restriction caused by blade trailing edge thickness. If there were no boundary layer, k_t for the rotor would be

$$k_{t_r} = k_t \quad \frac{A_2 + \Delta A_2}{A_2} \tag{37}$$

where ΔA_2 is the tip clearance area. However, experience has shown that there is some area restriction in ΔA_2 due to boundary layer buildup along the stationary walls. For this analysis it was assumed that the annulus area is increased by an amount equal to 0.5 (ΔA_2). The resulting expression for k_{t_r} is

$$K_{t_r} = \left[1 - \frac{2.7}{10^3}\left(\frac{t}{S}\ 100\right)^{3.3} \frac{a}{S}\right]\left(\frac{A_2 + 0.5\Delta A_2}{A_2}\right) \tag{38}$$

Expressions for W_{a_2} and ρ_2 must be obtained to solve Eq. (35). From the energy equation

$$\frac{W_2^2}{2gJc_p} = \frac{W_{a_2}^2 + W_{u_2}^2}{2gJc_p} = \eta_r \Delta T_{is} \tag{39}$$

Solving Eq. (39) for W_{a_2}

$$W_{a_2} = \left[2gJc_p \eta_r \Delta T_{is} - W_{u_2}^2 \right]^{1/2} \tag{40}$$

Combining Eqs. (32) and (40)

$$W_{a_2} = \left[2gJc_p \eta_r T_{t_E} \left(1 - \left(\frac{P_2}{P_{t_E}} \right)^{\frac{\gamma-1}{\gamma}} \right) - W_{u_2}^2 \right] \tag{41}$$

From the equation of state

$$\rho_2 = \frac{P_2}{RT_2}$$

Substituting Eq. (34) for T_2

$$\rho_2 = \frac{P_2}{RT_{t_E} \left\{ 1 - \eta_r \left[1 - \left(P_2 / P_{t_2} \right)^{\frac{\gamma-1}{\gamma}} \right] \right\}} \tag{42}$$

Substituting Eq. (40) and (42) into Eq. (35) for W_{a_2} and ρ_2

$$\frac{\dot{W}_t}{A_2 K_{t_r}} = \left(\frac{P_2}{RT_{t_E} \left\{ 1 - \eta_r \left[1 - \left(P_2 / P_{t_E} \right)^{\frac{\gamma-1}{\gamma}} \right] \right\}} \right) \left(2gJc_p \eta_r T_{t_E} \left[1 - \left(\frac{P_2}{P_{t_E}} \right)^{\frac{\gamma-1}{\gamma}} \right] - W_{u_2}^2 \right)^{1/2} \tag{43}$$

Rearranging Eq. (43)

$$\frac{\dot{W}_t \sqrt{T_{t_E}}}{P_2 A_2 K_{t_r}} \sqrt{\frac{R}{g} \frac{(\gamma-1)}{2\gamma}} = \frac{\left\{ \eta_r \left[1 - \left(\frac{P_2}{P_{t_E}} \right)^{\frac{\gamma-1}{\gamma}} \right] - \frac{W_{u_2}^2}{2gJc_p T_{t_E}} \right\}^{1/2}}{\left\{ 1 - \eta_r \left[1 - \left(\frac{P_2}{P_{t_E}} \right)^{\frac{\gamma-1}{\gamma}} \right] \right\}} \tag{44}$$

The left-hand side of Eq. (44) consists of known quantities and is a constant for a given set of operating conditions. Therefore, with

$$\frac{\dot{W}_t}{P_2 A_2 K_{t_r}} \sqrt{\frac{R}{g} \frac{(\gamma-1)}{2\gamma}} = K$$

and expanding Eq. (44)

$$\left[\eta_r - \frac{1}{2}\left(\frac{2K^2+1}{K^2\left[1-\left(P_2/P_{t_E}\right)^{\frac{\gamma-1}{\gamma}}\right]}\right)\right]^2 = \frac{1+4K^2\left(1-\frac{W_{u_2}^2}{2gJc_pT_{t_E}}\right)}{4K^2\left[1-\left(P_2/P_{t_E}\right)^{\frac{\gamma-1}{\gamma}}\right]^2} \quad (45)$$

Solving this quadratic equation for η_r yields

$$\eta_r = \frac{1+2K^2 \pm \sqrt{1+4K^2\left(1-\frac{W_{u_2}^2}{2gJc_pT_{t_E}}\right)}}{2K^2\left[1-\left(P_2/P_{t_E}\right)^{\frac{\gamma-1}{\gamma}}\right]} \quad (46)$$

By using an isentropic expansion from P_{tE} to p_2 for which the rotor efficiency would be equal to unity, it can be shown that the minus sign is applicable. With V_{u_2} known, there is

$$W_{u_2} = V_{u_2} - U_2$$

Therefore, all quantities on the right-hand side of Eq. (46) are known with the exception of the ratio p_2/P_{tE}. Multiplying both sides of Eq. (46) by the term containing this ratio, yields

$$\eta_r\left[1-\left(P_2/P_{t_E}\right)^{\frac{\gamma-1}{\gamma}}\right] = \frac{1+2K^2-\sqrt{1+4K^2\left(1-\frac{W_{u_2}^2}{2gJc_pT_{t_E}}\right)}}{2K^2} \quad (47)$$

Eq. (47) must be solved to obtain T_2. Substitution into Eq. (34) gives

$$T_2 = T_{t_E}\left[\frac{\sqrt{1+4K^2\left(1-\frac{W_{u_2}^2}{2gJc_pT_{t_E}}\right)}-1}{2K^2}\right] \quad (48)$$

With T_{t_E} and T_2 known

$$W_2 = \left[2gJc_p\left(T_{t_E} - T_2\right)\right]^{1/2} \tag{49}$$

Then

$$V_{a_2} = W_{a_2} = \left[W_2^2 - W_{u_2}^2\right]^{1/2}$$

and

$$V_2 = \left[V_{a_2}^2 + V_{u_2}^2\right]^{1/2}$$

The total temperature at the rotor exit may be found from

$$T_{t_2} = T_2 + \frac{V_2^2}{2gJc_p} = T_{tp1} - \frac{M_D \omega}{Jc_p \dot{W}_t} \tag{50}$$

where

ω = rotor speed (radians/sec)

The absolute and relative discharge angles are obtained from

$$\alpha_2 = \tan^{-1} \frac{V_{u_2}}{V_{a_2}} \qquad \text{(absolute flow)}$$

$$\beta_2 = \tan^{-1} \frac{W_{u_2}}{W_{a_2}} \qquad \text{(relative flow)}$$

Turbine Performance Analysis

In order to evaluate overall turbine performance additional parameters must be obtained.

The theoretical degree of reaction of a stage as defined by Vavra[18] is

$$r^* = \frac{h_1^* - h_2^*}{\Delta h_{is}} \tag{51}$$

r^* represents the ratio of the isentropic enthalpy drop in the rotor to the isentropic enthalpy drop in the stage. The degree of reaction is obtained at the hub, tip, and mean blade positions. With these data it is possible to ascertain which portions of the blade are performing as designed. Additionally, low values or r^* are indicative of small pressure drops through the rotor. For an axial turbine low values of r^* may result in decelerated flow in the rotor. This effect is illustrated in Fig. 14 where W_2 is less than W_1 even when the rotor losses are low.

The head coefficient defined by Vavra[19] is

$$k_{is} = \frac{\Delta h_{is}}{U_1^2/2gJ}$$

k_{is} is a dimensionless parameter relating the total isentropic enthalpy drop to the peripheral speed at the rotor entrance, and is an indication of the work capacity of a stage.

---

[18] Vavra, M. H., Aero-Thermodynamics and Flow in Turbomachines. (New York, London: John Wiley and Sons, Inc., 1960), Chap. 5, p. 422.

[19] Ibid., p. 426.

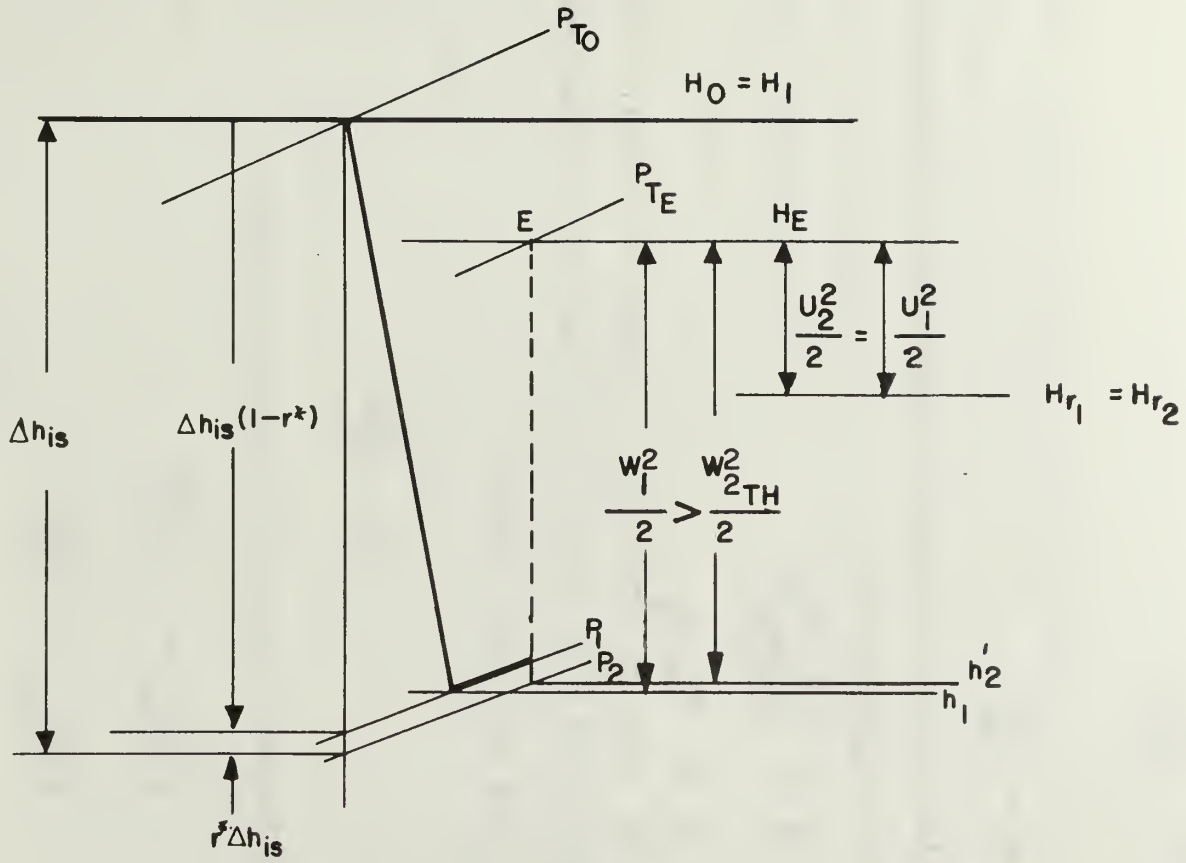

FIG. 14 EFFECTS OF LOW DEGREEOF REACTION ON AN AXIAL TURBINE

The power output of the turbine is measured by the dynamometer. The horsepower developed is then obtained from

$$HP = \frac{M_D \omega}{550}$$

where

$$\omega = N \frac{2\pi}{60}$$

All the desired output quantities are converted to referred values by using

$$\theta = \frac{\gamma R_g T_{tp1}}{\gamma R_g T_s} \qquad (52)$$

$$\delta = P_{tp1}/P_s$$

where T_s and p_s are 518.7 ^{o}R and 14.7 psia, respectively. Since the test fluid is air, and it is considered a perfect gas, Eq. (52) reduces to

$$\theta = \frac{T_{tp1}}{T_s}$$

Referred values of the data are then

$$(\dot{W}_t)_{ref} = \frac{\dot{W}_t \sqrt{\theta}}{\delta}$$

$$(M_D)_{ref} = \frac{M_D}{\delta}$$

$$(HP)_{ref} = \frac{HP}{\sqrt{\theta}\,\delta}$$

$$(N)_{ref} = \frac{N}{\sqrt{\theta}}$$

By using referred values, the data obtained at a given pressure ratio may be compared regardless of the inlet conditions.

Pressure and Velocity Surveys

The manometer readings taken during the surveys are used to obtain the total pressure, dynamic head, and pitch angle. The total pressure is obtained directly since it is compared to atmosphere at the manometer tube. The dynamic head is obtained from

$$q = p_1 - p_2$$

Calibration curves are provided with each probe by United Sensor and Control Corporation. These curves were used to obtain the pitch angle and Mach Number effects on the static pressure.

The recorded dynamic head had to be corrected for the above mentioned effects. Since the curves were given at relatively low Mach Numbers, extrapolation was necessary to obtain applicable corrections. Unfortunately, no definitive factors for the influence of immersion depth of the sensing holes were available.

5. Results and Discussion.

Each of the thirty test runs made was reduced with two different methods. Initially the data were reduced by using the momentum analysis outlined in Section 4. At that

time no attempt was made to satisfy continuity by the use of flow functions. Subsequently the same data were reduced by the analysis based on continuity which is described in the Appendix.

Comparison of the two methods indicated that the axial velocity at the stator discharge, obtained from the momentum analysis, was consistently higher than that obtained from continuity. Since the peripheral component of velocity is obtained in the same manner in both analyses, the resultant velocity obtained from momentum was also too high. The resulting stator loss coefficients were unrealistically low.

When using the momentum analysis, the axial velocity is a function of the axial forces on the stator assembly. All these forces are measured, with the exception of the pressure force acting on the stator blades. This force is determined from an assumed pressure distribution across the blade row. Initially the pressure was assumed to vary linearly from the stator hub to tip. When the velocities obtained with this pressure distribution were too high, a circular arc distribution was chosen in an attempt to obtain more realistic results. Although this pressure distribution yielded better results for the discharge velocities and angles, the resulting stator efficiencies were over one hundred percent.

In order to obtain more accurate pressure distributions at the stator discharge, flow surveys were made. Although

they were taken at several radial and peripheral positions, the results obtained were not conclusive. Only the discharge angles and total pressures could be considered correct. This was due to the probe calibration data which were available to obtain the static pressures. The available calibration curves hold for relatively low Mach Numbers, and had to be extrapolated for the data obtained in the present tests. The resulting corrections were of the order of twenty percent of the total reading.

These surveys did indicate however that the pressure variation from stator hub to tip was nearly linear. Fig. 15 shows the pressure distribution at the stator discharge. However, the pressure measured in the gap between the closure plate and the stator casing was significantly lower than that obtained from the survey data. This would indicate that, although a linear pressure distribution does exist, the net force obtained is higher than that obtained by using Eq. (4a).

It has already been noted that an increase in the force on the stator results in a stator efficiency of over 100 percent. However, from the total pressure survey ahead of the stator, it was found that the pressure indicated by the six fixed probes is lower than the average total pressure existing at the inlet. This results in an increase in the stator efficiency. The actual pressure distribution obtained from this survey is shown in Fig. 16.

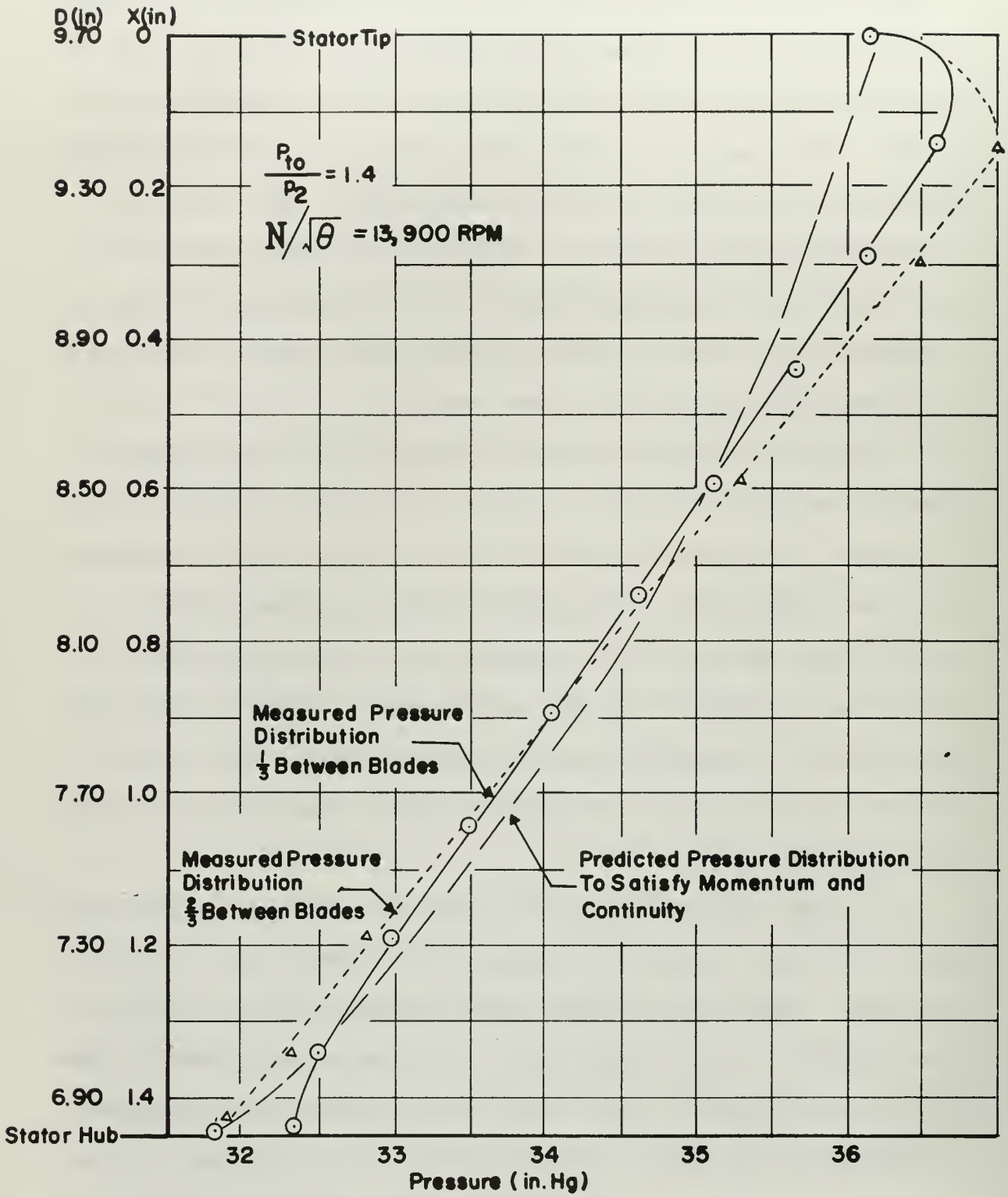

STATOR DISCHARGE SURVEY
FIG. 15

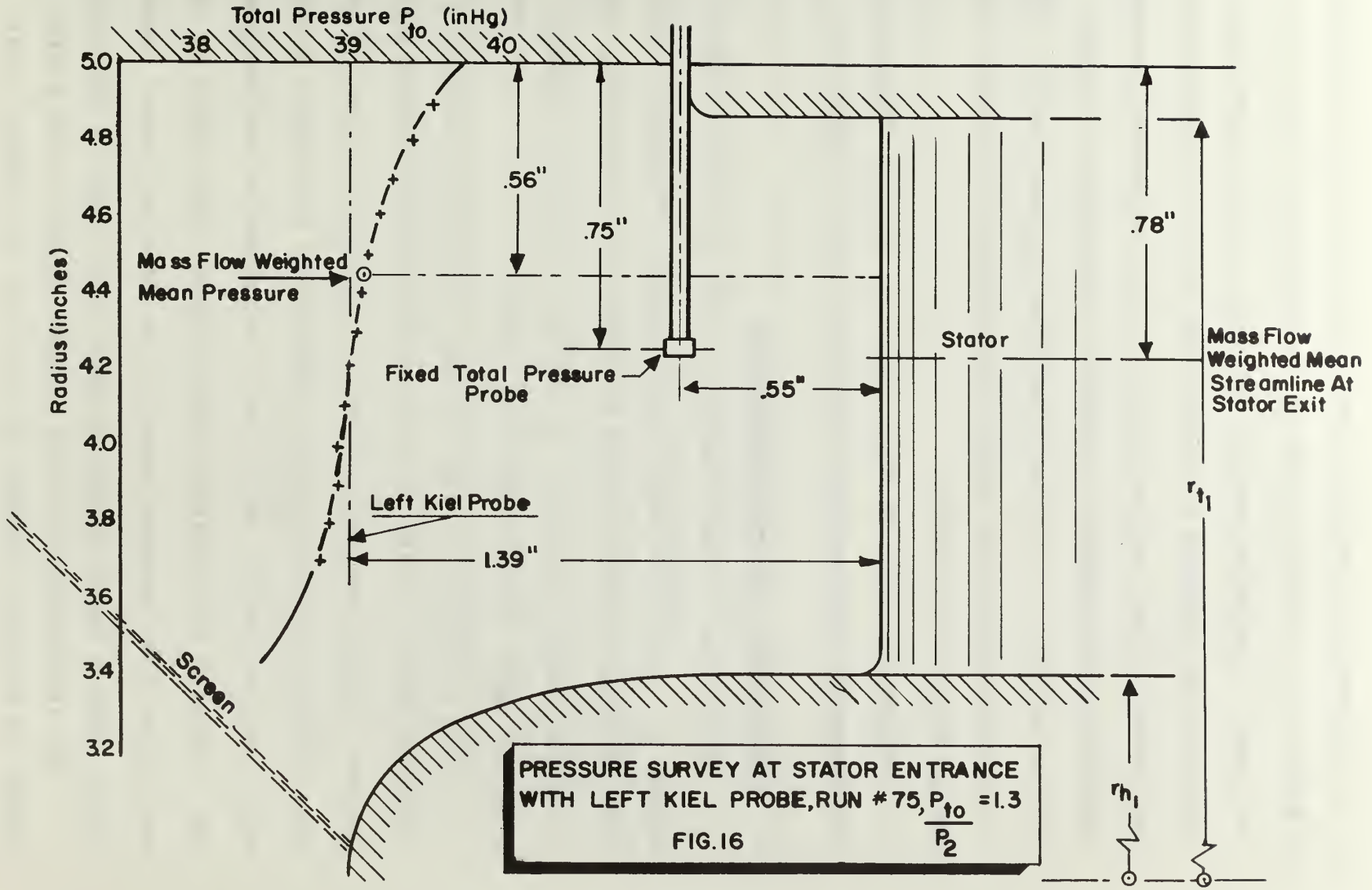

PRESSURE SURVEY AT STATOR ENTRANCE WITH LEFT KIEL PROBE, RUN #75, $\frac{P_{to}}{P_2}$ = 1.3

FIG. 16

The analysis shown in Section 4 was given to indicate a method that could be used if the pressure distribution at the stator discharge were not known. A linear pressure distribution was assumed to obtain the initial values and then the iteration was carried out to achieve agreement between continuity and momentum. However, this analysis failed for the majority of the data recorded in these tests. This is due to the low loss coefficients obtained from the momentum portion of the analysis.

Tables II, III, IV and V show the results obtained from the momentum and continuity analysis for run number 79.

6. Conclusions and Recommendations.

Variations in the pressure at the flow nozzle inlet affect all other readings significantly. Therefore, each item of data recorded should be taken at a particular value of nozzle inlet pressure. If average values of certain data are used, data scatter may result.

Data reduction by the methods outlined in Section 4 requires that all data be taken as accurately as possible. However, errors resulting from low indicated values of total inlet pressure will still be responsible for stator losses which are too small. Since this installation was designed for a turbine with smaller blade heights than those of the Mod II, the flow passage area of the floating stator assembly is almost equal to the annulus area ahead of the stator.

The installation of the screens ahead of the stator causes an entropy gradient to exist at the stator inlet.

Therefore, the assumption of uniform flow conditions is not valid. This difficulty could be overcome by increasing the size of the flow passage. The velocity in this region would then be reduced and the total pressure variation at the stator inlet would be reduced also. If the inlet total pressure is obtained accurately the method outlined in Section 4 will yield accurate results.

A further improvement could be made if the actual throat pressure were measured. This could be done by placing static taps at the hub, mean, and tip locations along a blade passage. Then the actual throat pressure could be used in the flow function rather than the stator discharge pressure. Fig. 17 is an illustration of how the pressure taps could be located at the throat passage.

Although it has been found that the stator discharge conditions may be predicted within three percent using a momentum analysis alone, it is felt that better results could be achieved with the analysis presented in Section 4, if the recommended changes in instrumentation were made.

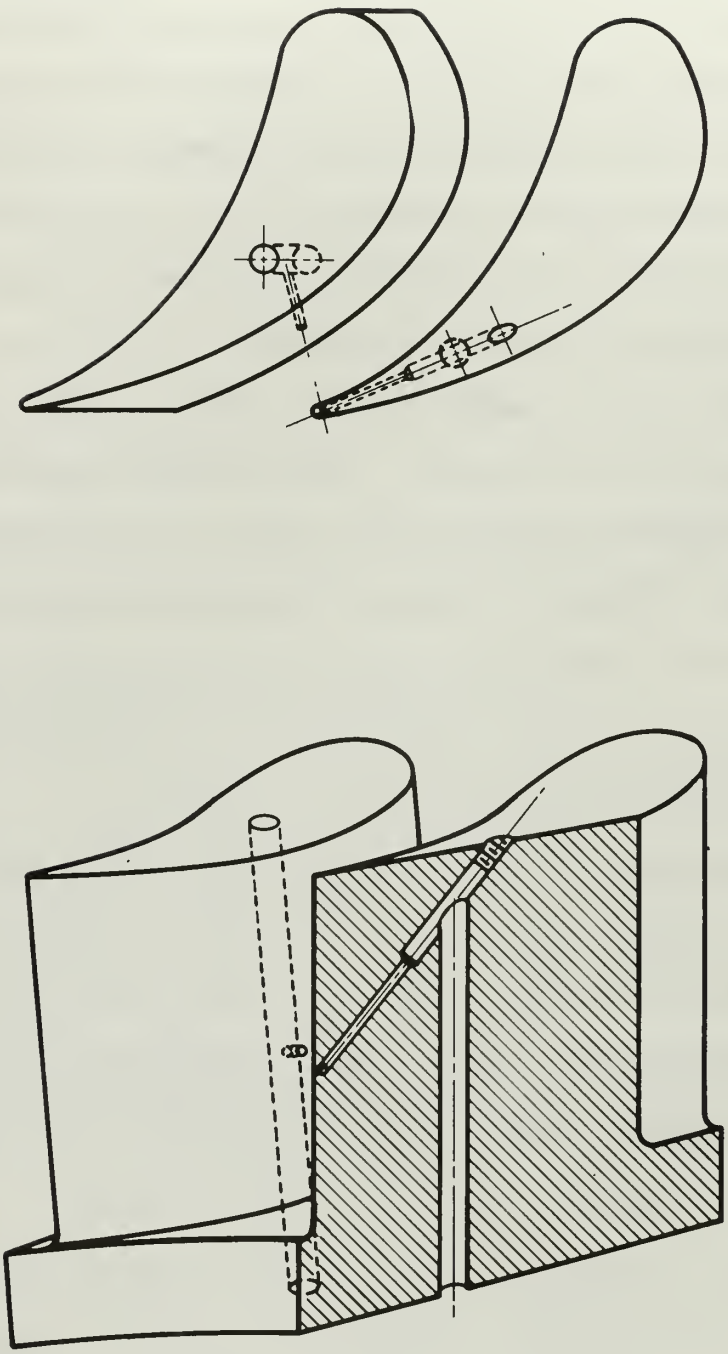

STATOR THROAT PRESSURE TAPS

FIG. 17

GENERAL RESULTS **CONTINUITY**

VELOCITIES (FT/SEC)
RUN NUMBER 79

POINT	V1	V2	W1	W2	U1
1	579.73145	201.66962	235.15054	391.20850	418.05078
2	576.14990	207.20213	222.46715	396.11133	437.78369
3	575.89014	217.74500	214.44550	393.60205	458.24805
4	574.88818	226.35335	207.20920	392.97559	474.32666
5	573.58521	238.50925	201.64336	394.10571	494.79102
6	574.13232	263.14331	201.76196	363.18286	495.52173

TEMPERATURES (DEG R)

POINT	PLENUM TOTAL	STATOR DISCHARGE	ROTOR DISCHARGE	ISENTROPIC FROM T1	TOTAL DISCHARGE
1	565.85156	537.88501	529.75366	526.49048	533.13794
2	565.68091	538.05884	529.12354	526.40503	532.69604
3	565.85156	538.25439	529.19263	526.41064	533.13794
4	565.85156	538.35034	529.07593	526.38867	533.33936
5	565.51025	538.13354	528.59619	525.99146	533.32983
6	565.68091	538.25195	530.66724	526.03784	536.42920

FLOW ANGLES (DEGREES FROM AXIAL) **CONTINUITY**

RUN NUMBER 79

PCINT	ALPHA 1	ALPHA 2	BETA 1	BETA 2	DELTA BETA
1	70.02647	21.72693	32.63414	-61.38754	94.02168
2	70.02522	25.36276	27.78581	-61.79211	89.57793
3	69.89960	30.90891	22.64500	-61.66359	84.30859
4	70.02046	34.56361	18.56224	-61.68404	80.24628
5	69.93495	38.34132	12.59791	-61.66217	74.26007
6	69.93703	44.53836	12.52937	-58.90594	71.43530

EFFICIENCIES AND LOSSES

PCINT	EFFICIENCY TOTAL STATIC	ZETA ROTOR	ZETA STATOR
1	0.80277	0.20385	0.04830
2	0.80739	0.17219	0.05517
3	0.80051	0.17734	0.05016
4	0.79334	0.17278	0.05345
5	0.78351	0.16754	0.05485
6	0.71133	0.29649	0.05231

TABLE III.

GENERAL RESULTS MOMENTUM

VELOCITIES (FT/SEC)
RUN NUMBER 79

POINT	V1	V2	W1	W2	U1
1	592.76221	201.66962	265.65869	391.20850	418.05078
2	586.11572	207.20213	247.13321	396.11133	437.78369
3	587.22534	217.74500	243.25128	393.60205	458.24805
4	587.01147	226.35335	238.79266	392.97559	474.32666
5	584.34204	238.50925	230.46890	394.10571	494.79102
6	585.39941	263.14331	231.88907	363.18286	495.52173

TEMPERATURES (DEG R)

POINT	PLENUM TOTAL	STATOR DISCHARGE	ROTOR DISCHARGE	ISENTROPIC FROM T1	TOTAL DISCHARGE
1	565.85156	536.61353	529.75366	525.24585	533.13794
2	565.68091	537.09497	529.12354	525.46191	532.69604
3	565.85156	537.15723	529.19263	525.33765	533.13794
4	565.85156	537.17822	529.07593	525.24268	533.33936
5	565.51025	537.09692	528.59619	524.97827	533.32983
6	565.68091	537.16479	530.66724	524.97534	536.42920

TABLE IV.

FLOW ANGLES (DEGREES FROM AXIAL) MOMENTUM

RUN NUMBER 79

POINT	ALPHA 1	ALPHA 2	BETA 1	BETA 2	DELTA BETA
1	66.80782	21.72693	28.51198	-61.38754	89.89952
2	67.49745	25.36276	24.81186	-61.79211	86.60397
3	67.06747	30.90891	19.84192	-61.66359	81.50551
4	66.98535	34.56361	16.03537	-61.68404	77.71941
5	67.22206	38.34132	11.00112	-61.66217	72.66328
6	67.10764	44.53836	10.88014	-58.90594	69.78609

EFFICIENCIES AND LOSSES

POINT	EFFICIENCY TOTAL STATIC	ZETA ROTOR	ZETA STATOR
1	0.80277	0.26132	0.00503
2	0.80739	0.21890	0.02220
3	0.80051	0.23006	0.01239
4	0.79334	0.22961	0.01311
5	0.78351	0.21853	0.01907
6	0.71133	0.34135	0.01474

TABLE V.

BIBLIOGRAPHY

1. Beer, R., Aerodynamic Design and Estimated Performance of a Two Stage Curtis Turbine for the Liquid Oxygen Turbopump of the M-1 Engine, NASA CR 54764 A6 C8800-12, 1965.

2. Eckert, R. H., Performance Analysis and Initial Tests of a Transonic Turbine Test Rig, Ae. Eng. Thesis, Naval Postgraduate School, Monterey, California, September 1967.

3. Flow Measurement, Chap. 4, Part 5, Supplement to Asme Power Test Codes, ASME, New York, New York, 1959.

4. Messegee, J. A., Influence of Axial and Radial Clearances on the Performance of a Turbine Stage with Blunt Edge Non-twisted Blades, Ae. Eng. Thesis, Naval Postgraduate School, Monterey, California, September 1967.

5. Monroe, P. A., An Investigation of the Performance and the Mixing Phenomena Associated with a Supersonic Exhauster Interacting with Subsonic Secondary Flow, Ae. Eng. Thesis, Naval Postgraduate School, Monterey, California, September 1967.

6. Naviaux, J. C., Transonic Turbine Test Rig Exhauster System Tests and Tests of a Reaction Turbine, M.Sc. Thesis, Naval Postgraduate School, Monterey, California December 1966.

7. Stearnes, R. F., et.al., Flow Measurement with Orifice Meters, Van Nostrand Co., Inc., New York, New York, 1951.

8. Vavra, M. H., Aero-Thermodynamics and Flow in Turbomachines, John Wiley and Sons, New York, New York 1960.

9. Vavra, M. H., Air Tests of the Ares Mod I Turbine, Report Ares VA-T, No. 8, 1966.

10. Vavra, M. H., Problems of Fluid Mechanics in Radial Turbomachines, Von Karman Institute Course Note 55a. Von Karman Institute for Fluid Dynamics, Rhode-Saint-Genese, Belgium, 1965.

APPENDIX

COMPUTER PROGRAM TO OBTAIN TURBINE PERFORMANCE

The computer program (TTR2) is composed of an executive routine and 11 subroutines. Two of these subroutines appear as subroutines of STATOR.

The comment cards give the program name, purpose, and indicate the units of each input item.

The executive routine reads the number of data sets to be reduced and provides the calling sequence for the subroutines. Any number of data sets may be reduced. However each set may consist of a maximum of 50 data points.

Subroutine INPUT is then called. This subroutine reads in the input data. The input data consist of the following entries:

Single Entries

1. Number of test run (NRUN)
2. Axial and radial clearance (AXCLR and RADCLR)
3. Barometric pressure
4. Number of data points
5. Temperatures in the Cascade Lab and Control Room

Multiple Entries

6. Pressure change across the flow nozzle
7. Total pressure flow nozzle
8. Total temperature, flow nozzle
9. Plenum total pressure-average of the six Kiel probes

10. Hub static pressure
11. Tip static pressure
12. Inlet total temperature
13. Reference pressure for, PNOZ, PHUB, PSPL, PHD
14. Rotational speed
15. Stator torque
16. Stator axial force
17. Dynamometer torque
18. Static pressure in hood-use p_{atm} when operating without the hood
19. Reference pressure for p_{tip}, p_{14-20}
20. Plenum static pressure
21. Closure plate axial force
22. Closure plate torque
23. Reference pressure for six plenum Kiel probes
24. Pressures around end of shroud

All pressures are entered as they are read on the manometer board with the exception of the actual pressure differential across the flow nozzle in inches of water (DH).

The multiple entries are entered with eight data points per card. After the input data have been read, they are printed out before exiting the subroutine.

In the following subroutine descriptions, the item numbers refer to the numbers listed on the left side of the enclosed print-out.

SETCON is the subroutine that establishes all the constants that are used in the program. All quantities in this subroutine have been discussed, with the exception of

item 30. This factor accounts for the effect of blade trailing edge thickness and will be used in the continuity analysis of STATOR.

Following SETCON, the input data are changed from subscripted to non-subscripted variables, which are denoted by Q. This is done to avoid the use of subscripts in all subroutines.

CONVERT is the subroutine that changes all units to a single system (psia, lb., ft., sec., ^{o}R). All areas remain in square inches.

Item 2 is the equation used to convert the temperatures, from millivolts, to degrees Rankine.

Item 3 is a conversion factor which accounts for the variation of water density due to temperature changes.

Items 5 and 8 are conversion factors which account for the temperature affects on the density of mercury.[20]

Items 26 through 29 depend on the calibration methods used to calibrate the torque and axial force on the stator assembly and closure plate.

Item 30 depends on the range over which the dynamometer is calibrated.

FLORAT is the subroutine which computes the turbine flowrate. The formula development is given in Section 3.

STATOR is the subroutine which computes the flow characteristics at the stator discharge. In this subroutine

---

[20] Stearnes, R. F., et. al., Flow Measurement with Orifice Meters (New York: Van Nostrand Co., Inc., 1951), p.261

either MOMENT or CONTIN is called to compute the absolute discharge velocity. The procedure followed in MOMENT has been outlined in Section 4. The continuity analysis is identical with that given in Section 4 for the rotor, with the exception that absolute velocities are used. The absolute velocity at the stator discharge is then obtained from

$$V_1 = \left[2gJc_p\left(T_{tp1} - T_1\right)\right]^{1/2}$$

where T_1 is obtained from

$$T_1 = \frac{T_{tp1}}{2K^2}\left\{\left[1 + 4K^2\left(1 - \frac{V_{u_1}^2}{2gJc_pT_{tp1}}\right)\right]^{1/2} - 1\right\}$$

with

$$K = \frac{\dot{w}_t\sqrt{T_{tp1}}}{A_1 K_{t_s} P_1}\sqrt{\frac{R}{g}\,\frac{\gamma-1}{2\gamma}}$$

Then

$$V_{a_1} = \sqrt{V_1^2 - V_{u_1}^2}$$

The other flow characteristics at the stator discharge are determined as shown in Section 4 under Stator Analysis.

ROTOR is the subroutine used to compute rotor exit conditions. The formula development for this subroutine may be found in Section 4 under Rotor Analysis.

PERFORM is the subroutine used to compute the various performance parameters outlined in Section 4 under Turbine Performance Analysis.

Following PERFORM, the executive routine converts the Q variables back into a one-dimensional array for output.

OUTPTA is a subroutine that gives a printout of all pertinent performance data. This printout consists of the following items:

1. Flow rate
2. RPM
3. Pressure ratio
4. Horsepower
5. k_{is}
6. Referred flow rate
7. Referred torque
8. Referred power
9. Referred speed
10. Absolute and relative discharge velocities and angles for the stator and rotor
11. Total plenum temperature
12. Static temperature at stator and rotor discharge
13. Static temperature achieved by an isentropic expansion from T_{tpl}
14. Total temperature at the rotor discharge
15. Flow deflection in the rotor ($\Delta\beta$)
16. Turbine efficiency (Total to static)
17. Rotor and stator loss coefficients
18. Degree of reaction at the hub, mean, and tip
19. Absolute and relative Mach Numbers at the stator discharge
20. Pressure ratio across the stator
21. Stator blockage factor (ξ_s)

OUTPUT prints out Items 3, 5, 17, 6, 7, 8, 9, 19 of OUTPTA in a report format. The turbine tested, radial and axial clearance, test run number, date of test, and data reduction method are given in the heading.

A sample program is shown in this appendix. Two stator subroutines are shown. The second contains the iterative process explained in Section 4.

```
C      PROGRAM TTR2_1
C      COMPUTES EXPERIMENTAL PERFORMANCE CHARACTERISTICS OF THE
C      TURBINE TEST RIG
C      INPUT DATA DH(IN H2O),PNOZ(IN HG),TNOZ(MV),PTPL(IN HG),PHUB(IN HG)
C      PTIP(IN HG),PBP(IN HG),TTPL(MV),PATM(IN HG),RPM(RPM),TORQR(COUNTS)
C      AXIL(COUNTS),DYNAR(COUNTS),PHD(IN HG),PRF1(IN HG),PSPL(IN HG),
C      CLAXIL(COUNTS),CLTRQR(COUNTS),PRF2(IN HG),THD(MV),P14 THRU P17
C      (IN HG),TCL(DEGREES F),TCR(DEGREES F).
0001        DIMENSION DH(50),PNOZ(50),TNOZ(50),PTPL(50),PHUB(50),PTIP(50),
           1PBP(50),TTPL(50),PATM(50),RPM(50),TORQR(50),AXIL(50),DYNAR(50),
           2PHD(50),PRF1(50),PSPL(50),CLAXIL(50), CLTRQR(50),PRF2(50)
           3,P18(50),P15(50),P16(50),P17(50),P19(50),P20(50)
0002        DIMENSION FLOWT(50),PR(50),HP(50),XKIS(50),COEFL(50),COEFM(50),
           1COEFP(50),COEFS(50),V1(50),V2(50),W1(50),W2(50),U1(50),U2(50),
           2T1(50),T2(50),T2IS(50),TT2(50),ALPH1(50),ALPH2(50),BETA1(50),
           3BETA2(50),DBETA(50),ETA(50),ETAT(50),ZETAR(50),ZETAS(50),ZETA(50),
           4REACHB (50),REACMN(50),REACTP (50),VM1(50),WM1(50),PHI(50),
           5          XI(50),PRS(50)
0003        COMMON G,CR,C2,C3,RM1,RM2,AAX,ATH,QFLOWT,QTTPL,T1IS,QT1,QPTPL,
           1QPTIP,QPHUB,P1,QP18,QP15,QP16,QP17,QPRS,TORQ,CLTORQ,QV1,VA1,VU1,
           2QZETAS,QPHI,QXI,GAM,QALPH1,QBETA1,QRPM,QU1,QW1,QVM1,QWM1,QPHD,
           3 CLFAX,FAX,RTIP1,RHUB1,SKT,PAMB,QP19,QP20
0004        READ 20,MM
0005     20 FORMAT(I10)
0006        DO 99 M=1,MM
0007        CALL INPUT(NRUN,AXCLR,RADCLR,PBAR,N,TCL,TCR,DH,PNOZ,TNOZ,PTPL,
           1PHUB,PTIP,    TTPL,PATM,RPM,TORQR,AXIL,DYNAR,PHD,PRF1,PSPL,
           2CLAXIL,CLTRQR,PRF2,P18,P15,P16,P17,P19,P20)
0008        CALL SETCON(BETA,CN,DN,AAX,AAXR,ATH,CR,GAM,G,CP,CJ,C1,C2,C3,C4,
           1C5,RTIP1,RHUB1,RTIP2,RHUB2,RM1,RM2,RADCLR,SKT,RKT)
0009        DO 90 I=1,N
0010        QDH=DH(I)
0011        QPNOZ=PNOZ(I)
0012        QTNOZ=TNOZ(I)
0013        QPTPL=PTPL(I)
0014        QPHUB=PHUB(I)
0015        QPTIP=PTIP(I)
0016        QPBP=PBP(I)
0017        QTTPL=TTPL(I)
0018        QPATM=PATM(I)
0019        QRPM=RPM(I)
0020        QTORQR=TORQR(I)
0021        QAXIL=AXIL(I)
0022        QDYNAR=DYNAR(I)
0023        QPHD=PHD(I)
0024        QPRF1=PRF1(I)
0025        QPSPL=PSPL(I)
0026        QCLXIL=CLAXIL(I)
```

```
0027              QLTRQR=CLTRQR(I)
0028              QPRF2=PRF2(I)
0029              QP18=P18(I)
0030              QP15=P15(I)
0031              QP16=P16(I)
0032              QP17=P17(I)
0033              QP19=P19(I)
0034              QP20=P20(I)
0035              CALL  CNVERT(QDH,QPNOZ,QTNOZ,QPTPL,QPHUB,QPTIP,     QTTPL,QPATM,
                 1QRPM,QTORQR,QAXIL,QDYNAR,QPHD,QPRF1,QPSPL, QLTRQR, QCLXIL,P1,P2,
                 2QP18,QP15,QP16,QP17,TORQ,CLTORQ,FAX,CLFAX,DYNA,PBAR,QPRF2,TCL,
                 3TCR,C5,PAMB,QP19,QP20)
0036              CALL FLORAT (CR,C5,DN,CN,BETA,QPNOZ,QPSPL,QTNOZ,QTTPL,QPHD,QDH,
                 1QFLOWT)
0037              CALL STATOR
0038              CALL ROTOR(G,CR,CP,CJ,C2,C3,RM1,RM2,AAXR,QFLOWT,QTTPL,QRPM,DYNA,
                 1QDP,P1,P2,QT1,QT2,QTT2,QT2IS,VA1,VU1,QV2,QW1,QW2,QU1,QU2,QALPH2,
                 2QBETA1,QBETA2,C4,RKT)
0039              CALL  PERFRM(G,CR,CP,C1,C2,C3,GAM,QTTPL,QPTPL,QPHUB,QPTIP,QPHD,
                 1QRPM,QFLOWT,DYNA,QDP,P2,T1IS,QT1,QT2IS,QPR,QETA,QXKIS,QCOEFL,
                 2QCOEFM,QCOEFP,QCOEFS, QEACMN,QEACHB ,QEACTP ,QZETAR,QALPH1,QALPH2,
                 3QBETA1,QBETA2,QDBETA,QHP,QU2,QW1,QW2)
0040              FLOWT(I)=QFLOWT
0041              PR(I)=QPR
0042              HP(I)=QHP
0043              XKIS(I)=QXKIS
0044              COEFL(I)=QCOEFL
0045              COEFM(I)=QCOEFM
0046              COEFP(I)=QCOEFP
0047              COEFS(I)=QCOEFS
0048              V1(I)=QV1
0049              V2(I)=QV2
0050              W1(I)=QW1
0051              W2(I)=QW2
0052              U1(I)=QU1
0053              U2(I)=QU2
0054              TTPL(I)=QTTPL
0055              T1(I)=QT1
0056              T2(I)=QT2
0057              T2IS(I)=QT2IS
0058              TT2(I)=QTT2
0059              ALPH1(I)=QALPH1
0060              ALPH2(I)=QALPH2
0061              BETA1(I)=QBETA1
0062              BETA2(I)=QBETA2
0063              DBETA(I)=QDBETA
0064              ETA(I)=QETA
0065              ZETAR(I)=QZETAR
```

```
0066                ZETAS(I)=QZETAS
0067                REACHB (I)=QEACHB
0068                REACMN(I)= QEACMN
0069                REACTP (I)=QEACTP
0070                VM1(I)=QVM1
0071                WM1(I)=QWM1
0072                PHI(I)=QPHI
0073                XI(I)=QXI
0074                PRS(I)=QPRS
0075                PTPL(I)=QPTPL
0076             90 CONTINUE
0077                CALL OUTPTA (NRUN,AXCLR,RADCLR,FLOWT,PR,HP,XKIS,COEFL,COEFM,COEFP,
                   1COEFS,V1,V2,W1,W2,U1,U2,T1,T2,T2IS,TT2,ALPH1,ALPH2,BETA1,BETA2,
                   2DBETA,ETA,     ZETAR,ZETAS,      REACHB ,REACMN,REACTP ,VM1,WM1,
                   3PHI,      XI,PRS,RPM,TTPL,N)
0078                CALL OUTPUT(NRUN,AXCLR,RADCLR,N,PR,XKIS,ETA,COEFL,COEFM,COEFP,
                   1COEFS,REACHB ,REACTP ,PTPL)
0079             99 CONTINUE
0080                END
```

```
0001            SUBROUTINE INPUT(NRUN,AXCLR,RADCLR,PBAR,N,TCL,TCR,DH,PNOZ,TNOZ,
               1PTPL,PHUB,PTIP,    TTPL,PATM,RPM,TORQR,AXIL,DYNAR,PHD,PRF1,PSPL,
               2CLAXIL, CLTRQR,PRF2,P18,P15,P16,P17,P19,P20)
0002            DIMENSION DH(50),PNOZ(50),TNOZ(50),PTPL(50),PHUB(50),PTIP(50),
               1       TTPL(50),PATM(50),RPM(50),TORQR(50),AXIL(50),DYNAR(50),
               2PHD(50),PRF1(50),PSPL(50),CLAXIL(50), CLTRQR(50),PRF2(50),
               3P18(50),P15(50),P16(50),P17(50),P19(50),P20(50)
0003            READ (5,101)NRUN
0004            READ (5,102)AXCLR,RADCLR
0005            READ (5,102)PBAR
0006            READ (5,101)N
0007            READ (5,102)TCL,TCR
0008            READ (5,102)(DH(I),I=1,N)
0009            READ (5,102)(PRF1(I),I=1,N)
0010            READ (5,102)(PTIP(I),I=1,N)
0011            READ (5,102)(P15 (I),I=1,N)
0012            READ (5,102)(P16 (I),I=1,N)
0013            READ (5,102)(P17 (I),I=1,N)
0014            READ (5,102)(P18 (I),I=1,N)
0015            READ (5,102)(P19 (I),I=1,N)
0016            READ (5,102)(P20 (I),I=1,N)
0017            READ (5,102)(PRF2(I),I=1,N)
0018            READ (5,102)(PTPL(I),I=1,N)
0019            READ (5,102)(PATM(I),I=1,N)
0020            READ (5,102)(PNOZ(I),I=1,N)
0021            READ (5,102)(PSPL(I),I=1,N)
0022            READ (5,102)(PHUB(I),I=1,N)
0023            READ (5,102)(PHD (I),I=1,N)
0024            READ (5,102)(TNOZ(I),I=1,N)
0025            READ (5,102)(TTPL(I),I=1,N)
0026            READ (5,102)(AXIL(I),I=1,N)
0027            READ (5,102)(TORQR(I),I=1,N)
0028            READ (5,102)(DYNAR(I),I=1,N)
0029            READ (5,102)(RPM(I),I=1,N)
0030            READ (5,102)(CLAXIL(I),I=1,N)
0031            READ (5,102)(CLTRQR(I),I=1,N)
0032            WRITE(6,105)NRUN,PBAR
0033            WRITE(6,107)(DH(I),I=1,N)
0034            WRITE(6,107)(PRF1(I),I=1,N)
0035            WRITE(6,107)(PTIP(I),I=1,N)
0036            WRITE(6,107)(P15(I),I=1,N)
0037            WRITE(6,107)(P16(I),I=1,N)
0038            WRITE(6,107)(P17(I),I=1,N)
0039            WRITE(6,107)(P18(I),I=1,N)
0040            WRITE(6,107)(P19(I),I=1,N)
0041            WRITE(6,107)(P20(I),I=1,N)
0042            WRITE(6,107)(PRF2(I),I=1,N)
0043            WRITE(6,107)(PTPL(I),I=1,N)
```

```
0044              WRITE(6,107)(PATM(I),I=1,N)
0045              WRITE(6,107)(PNOZ(I),I=1,N)
0046              WRITE(6,107)(PSPL(I),I=1,N)
0047              WRITE(6,107)(PHUB(I),I=1,N)
0048              WRITE(6,107)(PHD(I),I=1,N)
0049              WRITE(6,107)(TNOZ(I),I=1,N)
0050              WRITE(6,107)(TTPL(I),I=1,N)
0051              WRITE(6,107)(AXIL(I),I=1,N)
0052              WRITE(6,107)(TORQR(I),I=1,N)
0053              WRITE(6,107)(DYNAR(I),I=1,N)
0054              WRITE(6,107)(RPM(I),I=1,N)
0055              WRITE(6,107)(CLAXIL(I),I=1,N)
0056              WRITE(6,107)(CLTRQR(I),I=1,N)
0057            101 FORMAT(I10)
0058            102 FORMAT(8F10.4)
0059            105 FORMAT(1H1,//5X,11H RUN NUMBER,I5,//5X,40H INPUT DATA, CARD IMAGE,
                   1 1 LINE = 1 CARD //,5X,6H PBAR=,F6.3/)
0060            107 FORMAT(8F15.5)
0061                RETURN
0062                END
```

```
0001                SUBROUTINE SETCON(BETA,CN,DN,AAX,AAXR,ATH,CR,GAM,G,CP,CJ,C1,C2,
                   1C3,C4,C5,RTIP1,RHUB1,RTIP2,RHUB2,RM1,RM2,RADCLR,SKT,RKT)
0002                BETA=.533
0003                CN=1.05
0004                DN=4.25
0005                AAX=37.6499
0006                AAXR=41.7729
0007                ATH=12.70512
0008                CR=53.34
0009                GAM=1.401
0010                G=32.174
0011                CP=0.24
0012                CJ=778.16
0013                C1=2.*G*CJ
0014                C2=2.*G*CJ*CP
0015                C3=(GAM-1.)/GAM
0016                C4=1./C3
0017                C5=.0361269
0018                RTIP1=9.701/2.
0019                RHUB1=6.795/2.
0020                RTIP2=9.836/2.
0021                RHUB2=6.600/2.
0022                RM1=SQRT((RTIP1**2+RHUB1**2)/2.)
0023                RM2=SQRT((RTIP2**2+RHUB2**2)/2.)
0024                THKS=.048
0025                SSTAT=1.36378
0026                ASTAT=.4635
0027                THKR=.048
0028                SROTR=1.4343
0029                AROTR=.540
0030                SKT=1.-(2.7/1000.)*(THKS/SSTAT*100.)**3.3*ASTAT/SSTAT
0031                RKT=(1.-(2.7/1000.)*(THKR/SROTR*100.)**3.3*AROTR/SROTR)*((AAXR+
                   13.14159*RADCLR*(RTIP2+RADCLR/2.))/AAXR)
0032                RETURN
0033                END
```

```
0001              SUBROUTINE  CNVERT (DH,PNOZ,TNOZ,PTPL,PHUB,PTIP,     TTPL,PATM,RPM,
                 1TORQR,AXIL,DYNAR,PHD,PRF1,PSPL, CLTRQR,CLAXIL,P1,P2,P18,P15,P16,
                 2P17,TORQ,CLTORQ,FAX,CLFAX,DYNA,PBAR,PRF2,TCL,TCR,C5,PAMB,P19,P20)
0002              TEMP(X)=32.+35.98*X-.435*X**2
0003              GH2O=1.00013+TCR*.078/1000.-TCR**2.*.0014/1000.
0004              DH=DH*GH2O*C5
0005              CHGC=.49280-TCL*.5/10000.
0006              PAMB=PBAR
0007              PAMB=PAMB*CHGC
0008              CHGCR=.49280-TCR*.5/10000.
0009              PNOZ=CHGCR*(PATM-PNOZ)+PAMB
0010              PTPL=CHGCR*(PRF2-PTPL)+PAMB
0011              PHUB=CHGCR*(PATM-PHUB)+PAMB
0012              PTIP=CHGCR*(PRF1-PTIP)+PAMB
0013              P18=CHGCR*(PRF1-P18)+PAMB
0014              P15=CHGCR*(PRF1-P15)+PAMB
0015              P16=CHGCR*(PRF1-P16)+PAMB
0016              P17=CHGCR*(PRF1-P17)+PAMB
0017              P19=CHGCR*(PRF1-P19)+PAMB
0018              P20=CHGCR*(PRF1-P20)+PAMB
0019              PSPL=CHGCR*(PATM-PSPL)+PAMB
0020              PHD=CHGCR*(PATM-PHD)+PAMB
0021              EPS=0.0
0022              P1=((PTIP+PHUB)/2.)*(1.+EPS)
0023              P2=PHD
0024              TTPL= TEMP(TTPL)+459.7
0025              TNOZ= TEMP(TNOZ)+459.7
0026              TORQ=.3*TORQR/12.
0027              CLTORQ=.2207* CLTRQR/12.
0028              FAX=.08*AXIL
0029              CLFAX=CLAXIL
0030              DYNA=DYNAR/30.
0031              RETURN
0032              END
```

```
0001                SUBROUTINE FLORAT  (CR,C5,DN,CN,BETA,PNOZ,PSPL,TNOZ,TTPL,PHD,DH,
                   1FLOWT)
0002                ALPHN=1.+.00252*(TNOZ-527.7)/100.
0003                Z=1.9+.24*((TNOZ-459.7)/100.-1.)
0004                X=DH/PNOZ
0005                XR=1.-X
0006                B=(4.25/7.975)**4.
0007                Y=SQRT ((XR**(2./1.4))*3.5*(1.-XR**(.4/1.4))/(1.-XR)*(1.-B)/(1.
                   1-B*XR**(2./1.4)))
0008                FLOW=.8633*DN**2* ALPHN*CN*Y*SQRT (PNOZ*DH/TNOZ)
0009                PRL=PHD/PSPL
0010                FLOWS=SQRT ((1.-PRL)/4.0791)
0011                FLOWL=.116*FLOWS*PSPL/SQRT (TTPL)
0012                FLOWT=FLOW-FLOWL
0013                RETURN
0014                END
```

```
0001              SUBROUTINE STATOR
0002              COMMON G,CR,C2,C3,RM1,RM2,AAX,ATH, FLOWT, TTPL,T1IS, T1, PTPL,
                 1 PTIP, PHUB,P1, P18, P15, P16, P17, PRS,TORQ,CLTORQ, V1,VA1,VU1,
                 2 ZETAS, PHI, XI,GAM, ALPH1, BETA1, RPM, U1, W1, VM1, WM1, PHD,
                 3 CLEAX,EAX,RTIP1,RHUB1,SKT,PAMB,P19,P20
0003              PBAR=PAMB
0004              CALL CONTIN(G,C2,AAX,RM1,PHD,PTIP,P1,PHUB,P18,P15,P16,P17,FLOWT,
                 1TORQ,CLEAX,EAX,TTPL,VU1,VA1,V1,ALPH1,T1,RTIP1,RHUB1,CLTORQ,
                 2RADCLR,PBAR,DELP1,C3,SKT,CR,P19,P20)
0005              PRS=P1/PTPL
0006              T1IS=TTPL*PRS**C3
0007              ZETAS=(T1-T1IS)/(TTPL-T1IS)
0008              PHI=FLOWT/PTPL/ATH *SQRT (TTPL*CR/G)
0009           98 XI=PHI/SQRT(2./C3*(PRS**(2./GAM)-PRS**((GAM+1.)/GAM)))
0010              RAD=.10472*RPM
0011              U1=RM1*RAD/12.
0012              WU1=VU1-U1
0013              WA1=VA1
0014              BETA1=ATAN (WU1/WA1)
0015              W1=WA1/COS (BETA1)
0016              VM1=V1/SQRT (GAM*G*CR*T1)
0017              WM1=W1/SQRT (GAM*G*CR*T1)
0018              RETURN
0019              END
```

```
0001              SUBROUTINE STATOR
0002              COMMON G,CR,C2,C3,RM1,RM2,AAX,ATH, FLOWT, TTPL,T1IS, T1, PTPL,
                 1 PTIP, PHUB,P1, P18, P15, P16, P17, PRS,TORQ,CLTORQ, V1,VA1,VU1,
                 2 ZETAS, PHI, XI,GAM, ALPH1, BETA1, RPM, U1, W1, VM1, WM1, PHD,
                 3 CLFAX,FAX,RTIP1,RHUB1,SKT,PAMB,P19,P20
0003              PBAR=PAMB
0004              R=0.0
0005           97 EPS=R
0006              P1=((PHUB+PTIP)/2.)*(1.+EPS)
0007              CALL MOMENT(G,C2,AAX,RM1,PHD,PTIP,P1,PHUB,P18,P15,P16,P17,
                 1FLOWT,TORQ,CLFAX,FAX,TTPL,VU1,VA1,V1,ALPH1,T1,RTIP1,RHUB1,CLTORQ,
                 2RADCLR,PBAR,DELP1,C3,SKT,CR,EPS,P19,P20)
0008              PRS=P1/PTPL
0009              T1IS=TTPL*PRS**C3
0010              ZETAS=(T1-T1IS)/(TTPL-T1IS)
0011              PHI=FLOWT/PTPL/ATH *SQRT (TTPL*CR/G)
0012               POLY=GAM/(1.+ZETAS*(GAM-1.))
0013              PHIP=SQRT(2./C3*(PRS**(2./ POLY)-PRS**(( POLY+1.)/ POLY)))
0014              IF(ABS(PHI-PHIP)-0.001)98,98,99
0015           99 R=R+0.0001
0016              GO TO 97
0017           98 XI=PHI/SQRT(2./C3*(PRS**(2./GAM)-PRS**((GAM+1.)/GAM)))
0018              WRITE(6,995)EPS
0019          995 FORMAT(F10.4)
0020              RAD=.10472*RPM
0021              U1=RM1*RAD/12.
0022              WU1=VU1-U1
0023              WA1=VA1
0024              BETA1=ATAN (WU1/WA1)
0025              W1=WA1/COS (BETA1)
0026              VM1=V1/SQRT (GAM*G*CR*T1)
0027              WM1=W1/SQRT (GAM*G*CR*T1)
0028              RETURN
0029              END
```

```
0001                SUBROUTINE CONTIN(G,C2,AAX,RM1,PHD,PTIP,P1,PHUB,P18,P15,P16,P17,
                   1FLOWT,TORQ,CLFAX,FAX,TTPL,VU1,VA1,V1,ALPH1,T1,RTIP1,RHUB1,CLTORQ,
                   2RADCLR,PBAR,DELP1,C3,SKT,CR,P19,P20)
0002                VU1=(TORQ+CLTORQ)*G/FLOWT/RM1*12.
0003                THETA2=VU1**2./C2/TTPL
0004           .997 SK=FLOWT/SKT/AAX*SQRT (CR/G*C3/2.*TTPL)/P1
0005                T1=TTPL*(SQRT (1.+4.*SK**2*(1.-THETA2))-1.)/2./SK**2
0006                V1=SQRT ((TTPL-T1)*C2)
0007                VA1=SQRT (V1**2 -VU1**2 )
0008            999 ALPH1=ATAN (VU1/VA1)
0009                RETURN
0010                END
```

```
0001              SUBROUTINE MOMENT(G,C2,AAX,RM1,PHD,PTIP,P1,PHUB,P18,P15,P16,P17,
                 1FLOWT,TORQ,CLFAX,FAX,TTPL,VU1,VA1,V1,ALPH1,T1,RTIP1,RHUB1,CLTORQ,
                 2RADCLR,PBAR,DELP1,C3,SKT,CR,EPS,P19,P20)
0002              VU1=(TORQ+CLTORQ)*G/FLOWT/RM1*12.
0003              PI=3.14159
0004              A1=PI/4.*11.0**2
0005              A2=A1-PI/4.*10.132**2
0006              A2A=A1-A2-PI/4.*9.932**2
0007              A3=A1-PI/4.*(9.836+2.*RADCLR)**2.-A2-A2A
0008              A4=A1-A2-PI*RTIP1**2-A3-A2A
0009              A6=PI*RHUB1**2
0010              F1=A1*PHD
0011              F2=A2*(P19+P20)/2.
0012              F2A=A2A*(P17+P18)/2.
0013              F3=A3*(P15+P16)/2.
0014              F4=A4*PTIP
0015              F5=PI*(1+EPS)*(PHUB*(RTIP1**2-RHUB1**2)+2*((PTIP-PHUB)/(RTIP1-
                 1RHUB1))*(RTIP1**3/3.-RHUB1*RTIP1**2/2.+RHUB1**3/6.))
0016              F6=A6*PHUB
0017              FNET=F1-F2-F3-F4-F6+CLFAX+FAX-F2A-F5
0018               VA1=G*FNET/FLOWT
0019              ALPH1=ATAN (VU1/VA1)
0020              V1=SQRT (VA1**2+VU1**2)
0021              T1=TTPL-V1**2/C2
0022              RETURN
0023              END
```

```
0001              SUBROUTINE ROTOR(G,CR,CP,CJ,C2,C3,RM1,RM2,AAXR,FLOWT,TTPL,RPM,
                 1DYNA,DP,P1,P2,T1,T2,TT2,T2IS,VA1,VU1,V2,W1,W2,U1,U2,ALPH2,BETA1,
                 2BETA2,C4,RKT)
0002              RAD=.10472*RPM
0003              DP=DYNA*RAD/CJ
0004              VU2=RM1/RM2*VU1-DYNA*G/RM2/FLOWT*12.
0005              TT2=TTPL-DP/CP/FLOWT
0006              T2IS=T1*(P2/P1)**C3
0007              U2=RM2*RAD/12.
0008              WU2=VU2-U2
0009              TE=T1+(W1**2.-U1**2.+U2**2.)/C2
0010              TETA2=(WU2**2 )/TE/C2
0011              RK=FLOWT/RKT/AAXR*SQRT (CR/G*C3/2.*TE)/P2
0012              T2=TE*(SQRT (1.+4.*RK**2.*(1.-TETA2))-1.)/2./RK**2.
0013              V2=SQRT ((TT2-T2)*C2)
0014              VA2=SQRT(V2**2-VU2**2)
0015          615 WA2=VA2
0016              W2=SQRT (WA2**2+WU2**2)
0017              ALPH2=ATAN (VU2/VA2)
0018              BETA2=ATAN (WU2/WA2)
0019              RETURN
0020              END
```

```
0001              SUBROUTINE PERFRM  (G,CR,CP,C1,C2,C3,GAM,TTPL,PTPL,PHUB,PTIP,PHD,
                 1RPM,FLOWT,DYNA,DP,P2,T1IS,T1,T2IS,PR,ETA,XKIS,COEFL,COEFM,COEFP,
                 2COEFS,REACMN,REACHB ,REACTP ,ZETAR,ALPH1,ALPH2,BETA1,BETA2,DBETA,
                 3HP,U2,W1,W2)
0002              PR=PTPL/P2
0003              T2TH=TTPL*(PHD/PTPL)**C3
0004              DHIS=CP*(TTPL-T2TH)
0005              ETA=DP/DHIS/FLOWT
0006              XKIS=DHIS*C1/U2**2
0007              XKIS=XKIS*4.2048**2/4.125**2
0008              DEL=PTPL/14.69
0009              THETA=SQRT (GAM*CR*TTPL)/196.8107
0010              COEFL=FLOWT*THETA/DEL
0011              COEFM=DYNA/DEL
0012              HP=3600./2545.*DP
0013              COEFP=HP/(DEL*THETA)
0014              COEFS=RPM/THETA
0015              REACMN=1.0-CP*(TTPL-T1IS)/DHIS
0016              REACHB =((PHUB/PHD)**C3-1.)/((PTPL/PHD)**C3-1.)
0017              REACTP =((PTIP/PHD)**C3-1.)/((PTPL/PHD)**C3-1.)
0018              SQW2TH=C2*(T1-T2IS)+W1**2
0019              ZETAR=1.-W2**2/SQW2TH
0020              ALPH1=ALPH1*57.295779
0021              ALPH2=ALPH2*57.295779
0022              BETA1=BETA1*57.295779
0023              BETA2=BETA2*57.295779
0024              DBETA=BETA1-BETA2
0025              RETURN
0026              END
```

```
0001            SUBROUTINE OUTPTA (NRUN,AXCLR,RADCLR,FLOWT,PR,HP,XKIS,COEFL,COEFM,(
                1COEFP,COEFS,V1,V2,W1,W2,U1,U2,T1,T2,T2IS,TT2,ALPH1,ALPH2,BETA1,  (
                2BETA2,DBETA,ETA,     ZETAR,ZETAS,     REACHB ,REACMN,REACTP ,    (
                3VM1,WM1,PHI,     XI,PRS,RPM,TTPL,N)                            (
0002            DIMENSION FLOWT(50),PR(50),HP(50),XKIS(50),COEFL(50),COEFM(50),  (
                1COEFP(50),COEFS(50),V1(50),V2(50),W1(50),W2(50),U1(50),U2(50),  (
                2T1(50),T2(50),T2IS(50),TT2(50),ALPH1(50),ALPH2(50),BETA1(50),   (
                3BETA2(50),DBETA(50),ETA(50),ETAT(50),ZETAR(50),ZETAS(50),ZETA(50),(
                4REACHB (50),REACMN(50),REACTP (50),VM1(50),WM1(50),PHI(50),     (
                5          XI(50),PRS(50),RPM(50),TTPL(50)                       (
0003            WRITE(6,805)                                                     (
0004          805 FORMAT(1H1//22H ARES TURBINE MODEL II //)                      (
0005            WRITE(6,806)NRUN,AXCLR,RADCLR                                    (
0006          806 FORMAT(11H RUN NUMBER I3,8H SPACING F10.3,11H TIP CLEAR. F10.3/)
0007            WRITE(6,807)                                                     (
0008          807 FORMAT (5X,6H POINT  6X,10H FLOW RATE  9X,4H RPM
                1 5X,15H PRESSURE RATIO   5X,11H HORSEPOWER  /)
0009            DO 808 I=1,N
0010          808 WRITE(6,809)I,FLOWT(I),RPM(I),PR(I),HP(I)                      (
0011          809 FORMAT (I5,12X,4(F10.4,5X))
0012            WRITE(6,810)                                                     (
0013          810 FORMAT(///20X,37H DIMENSIONLESS PERFORMANCE PARAMETERS //
                15X, 6H POINT 11X, 2H K 10X, 9H REFERRED  8X, 9H REFERRED
                27X,9H REFERRED  7X,9H REFERRED  6X,      /
                317X,11H ISENTROPIC  5X,10H FLOW RATE  8X, 7H TORQUE
                4 9X, 6H POWER 10X, 6H SPEED  9X,/)
0014            DO 811 I=1,N
0015          811 WRITE(6,812)    I,XKIS(I),COEFL(I),COEFM(I),COEFP(I),COEFS(I)  (
0016          812 FORMAT ( I5,12X,6(F10.4,6X))
0017            WRITE(6,813)NRUN                                                 (
0018          813 FORMAT(1H1/////5X,16H GENERAL RESULTS //20X,20H VELOCITIES (FT/SEC
                1)/,20X,11H RUN NUMBER   I5/
                2//5X, 6H POINT 10X, 3H V1 12X, 3H V2 12X,3H W1 12X,3H W2
                312X,3H U1 12X,3H U2  /  )
0019            DO 814 I=1,N
0020          814 WRITE(6,815)   I,V1(I),V2(I),W1(I),W2(I),U1(I),U2(I)           (
0021          815 FORMAT ( I5,12X, 6(F10.5,5X))
0022            WRITE(6,816)                                                     (
0023          816 FORMAT (       /20X,23H TEMPERATURES (DEG R )  //
                1 5X, 6H POINT   8X, 7H PLENUM  6X, 7H STATOR  8X, 6H ROTOR
                2 9X,11H ISENTROPIC   4X, 6H TOTAL  /19X, 6H TOTAL  7X,
                310H DISCHARGE  5X,10H DISCHARGE  5X, 8H FROM T1  7X,
                410H DISCHARGE / )
0024            DO 817 I = 1,N
0025          817 WRITE(6,818)      I, TTPL(I), T1(I), T2(I), T2IS(I), TT2(I)    (
0026          818 FORMAT ( I5,12X, 5(F10.5,5X))
0027            WRITE(6,819)NRUN                                                 (
0028          819 FORMAT(1H1/////20X,33H FLOW ANGLES (DEGREES FROM AXIAL)  //
```

```
     120X,11H RUN NUMBER    I5///
     2 5X, 6H POINT    7X, 8H ALPHA 1  8X, 8H ALPHA 2  7X, 7H BETA 1
     3 8X, 7H BETA 2   6X,12H DELTA BETA  / )
0029       DO 820 I=1,N
0030   820 WRITE(6,821) I, ALPH1(I),ALPH2(I),BETA1(I),BETA2(I),DBETA(I)
0031   821 FORMAT ( I5,12X, 5(F10.5,5X))
0032       WRITE(6,822)
0033   822 FORMAT (       ///20X,24H EFFICIENCIES AND LOSSES    //
     12X,6H POINT 10X, 11H EFFICIENCY 17X, 5H ZETA 20X, 5H ZETA/
     217X, 13H TOTAL STATIC 16X, 6H ROTOR 18X, 7H STATOR/)
0034       DO 823 I=1,N
0035   823 WRITE(6,824)   I,ETA(I),ZETAR(I),ZETAS(I)
0036   824 FORMAT (I5,12X,3(F10.5,15X))
0037       WRITE(6,825)NRUN
0038   825 FORMAT  (1H1,36H MACH NUMBERS AND DEGREE OF REACTION   //
     120X,11H RUN NUMBER    I5///
     25X,6H POINT  8X,9H REACTION  6X,9H REACTION  7X,9H REACTION
     37X,9H ABSOLUTE  7X,9H RELATIVE  / 23X,4H HUB  9X,5H MEAN  11X,
     44H TIP  12X,7H MACH 1  9X,7H MACH 1   //)
0039       DO 826 I=1,N
0040   826 WRITE(6,827) I,REACHB (I),REACMN(I),REACTP (I),VM1(I),WM1(I)
0041   827 FORMAT  (I5,12X,5(F10.4,6X))
0042       WRITE(6,828)
0043   828 FORMAT (//49H STATOR PRESSURE RATIO AND THROAT BLOCKAGE FACTOR//
     12X,6H POINT 11X,9H PRESSURE 17X,9H BLOCKAGE /
     221X,6H RATIO 19X,7H FACTOR /)
0044       DO 829 I=1,N
0045   829 WRITE(6,830) I,PRS(I),XI(I)
0046   830 FORMAT(I5,12X,2(F10.5,15X))
0047       RETURN
0048       END
```

```
0001            SUBROUTINE OUTPUT(NRUN,AXCLR,RADCLR,N,PR,XKIS,EFF,COEFL,COEFM,
               1                  COEFP,COEFS,REACHB ,REACTP ,PTPL)
0002            DIMENSION PR(50),XKIS(50),EFF(50),COEFL(50),COEFM(50),COEFP(50),
               1          COEFS(50),REACHB (50),REACTP (50),PTPL(50),NPTS(8),
               2          NPTSS(8),ICOEFS(50)
0003            READ(5,905)DATE
0004            READ(5,906)  REPRTA ,REPRTB ,TTYPEA,TTYPEB,CONFIG,METHOD
0005            READ(5,907)RMEAN
0006            READ(5,908)J
0007            READ(5,909)  (NPTS(K),NPTSS(K),K=1,8)
0008            DO 919 I=1,N
0009          919 EFF(I)=100.*EFF(I)
0010            DO 950 JJ=1,2
0011            IF (N+3*J-43) 920,920,921
0012          920 NPP=1
0013            NXX=N
0014            GO TO 922
0015          921 NPP=2
0016            NXX=43
0017          922 NP=1
0018            NX=1
0019            K=1
0020          923 WRITE(6,900)  REPRTA ,REPRTB ,NP,NPP,TTYPEA,TTYPEB,CONFIG,RADCLR,
               1              AXCLR,NRUN,DATE,METHOD
0021            WRITE(6,901)RMEAN
0022            DO 940 I=NX,NXX
0023            ICOEFS(I)=COEFS(I)
0024            II=I
0025            WRITE(6,902)  I,PR(I),XKIS(I),EFF(I),COEFL(I),COEFM(I),COEFP(I),
               1              ICOEFS(I),REACHB (I),REACTP (I)
0026            IF (J-K) 940,924,924
0027          924 IF (I-NPTSS(K)) 940,925,940
0028          925 LL=NPTS(K)
0029            LLL=NPTSS(K)
0030            INTGER =LLL-LL+1
0031            AVG=INTGER
0032            AVGATM=0.0
0033            AVGPR=0.0
0034            DO 926 L=LL,LLL
0035            AVGATM=AVGATM+PTPL(L)/14.69 /AVG
0036          926 AVGPR=AVGPR+PR(L)/AVG
0037            LLL=LLL-1
0038            COMPAR =PR(LL)
0039            DO 931 L=LL,LLL
0040            IF (COMPAR -PR(L+1)) 930,931,931
0041          930 COMPAR =PR(L+1)
0042          931 CONTINUE
0043            DEVHI  =100.*(COMPAR -AVGPR)/AVGPR
```

```
0044              COMPAR =PR(LL)
0045              DO 934 L=LL,LLL
0046              IF (COMPAR -PR(L+1)) 934,934,933
0047          933 COMPAR =PR(L+1)
0048          934 CONTINUE
0049              DEVLOW=100.*(AVGPR-COMPAR )/AVGPR
0050              WRITE(6,903)  NPTS(K),NPTSS(K),AVGPR,DEVHI   ,DEVLOW,AVGATM
0051              IF (NPTSS(K+1)+3*(K+1)-43) 936,936,935
0052          935 IF (NP-2) 944,936,944
0053          936 K=K+1
0054          940 CONTINUE
0055          944 IF (N-II) 950,950,945
0056          945 K=K+1
0057              NP=2
0058              NX=II+1
0059              NXX=N
0060              WRITE(6,904)NP
0061              GO TO 923
0062          900 FORMAT(1H1,/ ,9X,7H REPORT,2X,A8,A2,77X,6H SHEET,1X,I1,3H OF,1X,I1
                  1,//,33X,53H TURBO PROPULSION LABORATORY USNPGS, MONTEREY, CALIF. ,
                  2///,21X,79H REDUCED PERFORMANCE DATA OF TURBINE FROM TESTS WITH TR
                  3ANSONIC TURBINE TEST RIG // ,13H TURBINE TYPE,1X,A8,A3,14H CONFIGU
                  4RATION,1X,A5,1X,25H RADIAL ROTOR TIP CLEAR.=,2X,F4.3,32H IN.  AXIA
                  5L CLEAR. STATOR-ROTOR=,1X,F5.3,4H IN./ ,24X,13H TEST RUN NO.,1X,I3
                  6,3X,13H DATE OF TEST,1X,A8,2X,22H DATA REDUCTION METHOD,1X,A4 // )
0063          901 FORMAT(7X,105H POINT  PRESSURE   ISENTROPIC   EFFICIENCY  REFERRED
                  1   REFERRED  REFERRED  REFERRED  DEGREE OF  DEGREE OF / ,15X, 96H
                  2RATIO     HEAD COEFF.  TOT-STATIC  FLOW RATE   TORQUE    POWER
                  3 SPEED    REACTION   REACTION / ,24X, 4H (R=,   F5.3,77H IN.)  PER
                  4CENT     LBM/SEC    FT-LB      HP         RPM      (HUB)      (TIP)
                  5  //)
0064          902 FORMAT(9X,I2,5X,F6.4,5X,F6.4,8X,F5.2,6X,F6.4,5X,F6.3,4X,F6.3,4X,
                  1I5,5X,F5.4,6X,F5.4 )
0065          903 FORMAT(/5X,12H FOR POINTS , I2,3H TO,1X,I2,21H AVG. PRESSURE RATIO
                  1=,1X,F6.4,18H , MAX.DEVIATION +,   F5.3,7H PCT. -,   F5.3,19H PCT.
                  2, PAVG./PATMO=,1X,F6.4 /)
0066          904 FORMAT(/45X,16H CONTD. ON SHEET,1X,I1,/)
0067          905 FORMAT(A8)
0068          906 FORMAT(A8,A2,10X,A8,A3,9X,A5,5X,A4)
0069          907 FORMAT(F5.3)
0070          908 FORMAT(I1)
0071          909 FORMAT(8(2I5))
0072          950 CONTINUE
0073              RETURN
0074              END
```

RUN NUMBER 79

INPUT DATA, CARD IMAGE, 1 LINE = 1 CARD

PBAR=30.050

37.89999	37.59999	37.70000	37.59999	37.59999	37.59999
50.00000	50.00000	50.00000	50.00000	50.00000	50.00000
46.03000	45.96999	45.90999	45.87999	45.81999	45.79999
50.26999	50.25999	50.25000	50.23999	50.23000	50.20999
50.28999	50.28000	50.26999	50.26999	50.26999	50.25000
50.25000	50.25000	50.23999	50.23000	50.23000	50.23000
50.12000	50.12000	50.10999	50.10999	50.12000	50.12000
50.01999	50.01999	50.00999	50.00999	50.01999	50.00999
50.01999	50.01999	50.01999	50.01999	50.01999	50.01999
50.00000	50.00000	50.00000	50.00000	50.00000	50.00000
41.00000	40.96999	40.96999	40.93999	40.90999	40.89999
70.00000	70.00000	70.00000	70.00000	70.00000	70.00000
48.89999	48.89999	48.89999	48.89999	48.89999	48.89999
52.64999	52.64999	52.64999	52.64999	52.64999	52.64999
69.29999	69.25000	69.23000	69.20999	69.18999	69.17999
70.00000	70.00000	70.00000	70.00000	70.00000	70.00000
2.19500	2.19500	2.19500	2.19500	2.17500	2.17000
2.11500	2.11000	2.11500	2.11500	2.10500	2.11000
955.00000	960.00000	975.00000	983.00000	987.00000	988.00000
899.00000	890.00000	890.00000	888.00000	886.00000	887.00000
589.00000	565.00000	536.00000	514.00000	488.00000	443.00000
11440.00000	11980.00000	12540.00000	12980.00000	13540.00000	14560.00000
12.06000	12.44000	13.04000	13.31000	13.75000	14.38000
15.00000	15.00000	15.00000	15.00000	15.00000	15.00000

INITIAL DISTRIBUTION LIST

		No. Copies
1.	Defense Documentation Center Cameron Station Alexandria, Virginia 22314	20
2.	Library U. S. Naval Postgraduate School Monterey, California 93940	2
3.	Commander, Naval Air Systems Command Navy Department Washington, D. C. 20360	1
4.	Commander, Naval Ship Systems Command Navy Department Washington, D. C. 20360	1
5.	Capt. A. Bodnaruk, USN Naval Ship Systems Command (Code 6140) Navy Department Washington, D. C. 20360	1
6.	Office of Naval Research (Power Branch) Attn. Mr. J. K. Patton, Jr. Navy Department Washington, D. C. 20360	1
7.	Mr. R. Beichel Liquid Rocket Plant Aerojet-General Corporation Sacramento, California 95809	1
8.	Chairman, Department of Aeronautics U. S. Naval Postgraduate School Monterey, California 93940	2
9.	Professor M. H. Vavra Department of Aeronautics U. S. Naval Postgraduate School Monterey, California 93940	3
10.	Lt. P. M. Commons, USN VA 122 NAS Lemoore Lemoore, California	3

DOCUMENT CONTROL DATA - R&D

(Security classification of title, body of abstract and indexing annotation must be entered when the overall report is classified)

1. ORIGINATING ACTIVITY *(Corporate author)*
Naval Postgraduate School
Monterey, California 93940

2a. REPORT SECURITY CLASSIFICATION
UNCLASSIFIED

2b. GROUP

3. REPORT TITLE

4. DESCRIPTIVE NOTES *(Type of report and inclusive dates)*
Thesis, M.S., September 1967

5. AUTHOR(S) *(Last name, first name, initial)*
Commons, Patrick M., LT, USN

6. REPORT DATE	7a. TOTAL NO. OF PAGES	7b. NO. OF REFS
September 1967	108	10

8a. CONTRACT OR GRANT NO.	9a. ORIGINATOR'S REPORT NUMBER(S)
b. PROJECT NO.	
c.	9b. OTHER REPORT NO(S) *(Any other numbers that may be assigned this report)*

11. SUPPLEMENTARY NOTES	12. SPONSORING MILITARY ACTIVITY
	Commander Naval Air Systems Command Department of the Navy Washington, D. C. 20360

13. ABSTRACT

The primary purpose of the Transonic Turbine Test Rig is to study the effects of axial and radial clearances on turbine performance. Additionally, the installation was designed to permit the determination of stator discharge velocities by the application of the momentum, and moment of momentum equations.

Previous attempts to obtain stator discharge velocities by these methods have been unsuccessful. However, during this series of tests, with over 150 hours of useful operating time, the instrumentation and the data acquisition procedures were improved to the extent that the difference between stator discharge velocities obtained from a momentum analysis and those obtained from continuity were reduced to less than three percent.

DD FORM 1 JAN 64 1473

14. KEY WORDS	LINK A		LINK B		LINK C	
	ROLE	WT	ROLE	WT	ROLE	WT
Turbine Instrumentation						
Turbine Test Rig						
Inlet Guide Vanes						
Momentum Equation						
Moment of Momentum Equation						